Journal of Medicinal Chemistry

Subscriber access provided by Kaohsiung Medical University

Article

# Structural insights of benzene sulfonamide analogs as NLRP3 inflammasome inhibitors: Design, synthesis, and biological characterization

Jacob W Fulp, Liu He, Stefano Toldo, Yuqi Jiang, Ashley Boice, Chunqing Guo, Xia Li, Andrew Rolfe, Dong Sun, Antonio Abbate, Xiang-Yang Wang, and Shijun Zhang

*J. Med. Chem.*, **Just Accepted Manuscript** • DOI: 10.1021/acs.jmedchem.8b00733 • Publication Date (Web): 07 Jun 2018

**Downloaded from http://pubs.acs.org on June 7, 2018**

## Just Accepted

"Just Accepted" manuscripts have been peer-reviewed and accepted for publication. They are posted online prior to technical editing, formatting for publication and author proofing. The American Chemical Society provides "Just Accepted" as a service to the research community to expedite the dissemination of scientific material as soon as possible after acceptance. "Just Accepted" manuscripts appear in full in PDF format accompanied by an HTML abstract. "Just Accepted" manuscripts have been fully peer reviewed, but should not be considered the official version of record. They are citable by the Digital Object Identifier (DOI®). "Just Accepted" is an optional service offered to authors. Therefore, the "Just Accepted" Web site may not include all articles that will be published in the journal. After a manuscript is technically edited and formatted, it will be removed from the "Just Accepted" Web site and published as an ASAP article. Note that technical editing may introduce minor changes to the manuscript text and/or graphics which could affect content, and all legal disclaimers and ethical guidelines that apply to the journal pertain. ACS cannot be held responsible for errors or consequences arising from the use of information contained in these "Just Accepted" manuscripts.

ACS Publications

is published by the American Chemical Society. 1155 Sixteenth Street N.W., Washington, DC 20036

Published by American Chemical Society. Copyright © American Chemical Society. However, no copyright claim is made to original U.S. Government works, or works produced by employees of any Commonwealth realm Crown government in the course of their duties.

# Structural insights of benzene sulfonamide analogs as NLRP3 inflammasome inhibitors: Design, synthesis, and biological characterization

Jacob Fulp[a], Liu He[a], Stefano Toldo[b], Yuqi Jiang[a], Ashley Boice[a], Chunqing Guo[c], Xia Li[c], Andrew Rolf[d], Dong Sun[d], Antonio Abbate[b], Xiang-Yang Wang[c], Shijun Zhang[a]*

[a]*Department of Medicinal Chemistry* , [b]*Department of Internal Medicine and Pauley Heart Center,* [c]*Department of Human & Molecular Genetics,* [d]*Department of Anatomy and Neurobiology, Virginia Commonwealth University, Richmond, Virginia, USA, 23298*

**Abstract**

NLRP3 inflammasome plays critical roles in a variety of human diseases and represents a promising drug target. In this study, we established the *in vivo* functional activities of **JC124**, a previously identified NLRP3 inflammasome inhibitor from our group, in mouse models of Alzheimer's disease and acute myocardial infarction. To understand the chemical space of this lead structure, a series of analogs were designed, synthesized, and biologically characterized. The results revealed the critical roles of the two substituents on the benzamide moiety of **JC124**. On the other hand, modifications on the sulfonamide moiety of **JC124** are well tolerated. Two new lead compounds, **14** and **17**, were identified with improved inhibitory potency ($IC_{50}$ of 0.55 ± 0.091 and 0.42 ± 0.080 μM, respectively). Further characterization confirmed their selectivity and *in vivo* target engagement. Collectively, the results strongly encourage further development of more potent analogs based on this chemical scaffold.

**Introduction**

Inflammasomes are intracellular multiprotein complexes that tightly regulate the innate immune response and the production of pro-inflammatory cytokines such as interleukin (IL)-1β and IL-18.[1] The inflammasomes share a similar structure and are typically formed by a sensor component, an adaptor component (the apoptosis-associated speck-like protein containing a caspase recruitment domain---ASC), an effector component, typically pro-caspase-1, and the substrate component (the pro-inflammatory cytokines IL-1β and IL-18).[2,3] The sensors recognize danger signals such as *Damage associated molecular pattern molecules* (DAMPs) released during tissue injury or stress (extracellular ATP, urate crystal, β-amyloid, cell debris, etc) and *Pathogen-associated molecular patterns* (PAMPs), evolutionary conserved structures of the

microbial invader. Upon assembly of the inflammasome complex, pro-caspase-1 will be cleaved and activated to process proinflammatory cytokines IL-1β and IL-18 to their active forms, then mediating a plethora of inflammatory responses and ultimately to one specific cell death known as pyroptosis.[3,4]

A number of inflammasome complexes have been identified and this includes the NOD-like receptor (NLR) containing family such as NLRP1, NLRP3, NLRP6, NLRP7, NLRP12, NLRC4, the absent in melanoma 2 (AIM2) inflammasome, and retinoic acid-inducible gene I (RIG-I) like receptors (RLRs).[3] Among these, the NLRP3 inflammasome, which is composed of the sensor NLRP3, the adapter ASC, and pro-caspase-1, has been extensively studied and is critically involved in the maturation of IL-1β and IL-18.[1] Most recently, a new player, NEK7, has been added to the NLRP3 inflammasome complex as an essential component to its activation.[5-7] Emerging evidence has suggested critical roles for the NLRP3 inflammasome and IL-1β in the pathogenesis of many human diseases, such as autoinflammatory disorders, diabetes, acute myocardial infarction (AMI), traumatic brain injury (TBI), multiple sclerosis (MS), and Alzheimer's disease (AD).[8-20] The pathological roles of the NLRP3 inflammasome are well illustrated by cryopyrin-associated periodic syndrome (CAPS), a group of inherited autoinflammatory diseases, caused by gain-of-function mutations in the NLRP3 protein.[9] Recently, studies have demonstrated that levels of IL-1β and expression of active caspase-1 were found to be elevated in AD mouse models and AD patients.[13, 17, 18, 21, 22] Notably, $NLRP3^{-/-}$ and $Casp^{-/-}$ mice carrying mutations associated with familial AD exhibited improved cognitive functions, thus clearly suggesting the essential roles of the NLRP3 inflammasome axis in AD development.[17] Most recently, ASC specks derived from microglia has been shown to cross seed amyloid-β (Aβ) in transgenic AD mice, thus support the

role of NLRP3 inflammasome activation in driving the Aβ pathology of AD.[20] NLRP3 inflammasome also plays critical roles in the inflammatory responses to myocardial injury during AMI.[23] In the early phases of AMI, the acute ischemic injury induces the expression of NLRP3 inflammasome components (*priming)*, which concomitantly provides the stimuli leading to NLRP3 activation and formation of the macromolecular aggregate (*trigger)*, leading to an active inflammasome.[23,24] Caspase-1 is detected in the heart starting 3 to 6 hours after ischemia and its activity peaks between 24 and 72 hours, while low grade activation persists for weeks after the initial insult.[23,25] Reperfusion, while it effectively reduces infarct size, does not prevent activation of the NLRP3 inflammasome and leads to further injury through caspase-1-dependent inflammatory cell death.[26] To support this notion, studies by Abbate and others demonstrated that mice with genetic deletion of NLRP3 or ASC exhibited smaller infarct size in experimental AMI model, and reduced tendency toward adverse remodeling and heart failure, consistent with previously reported central role of caspase-1 in AMI.[25,27,28] Transgenic mice expressing constitutively active caspase-1, on the other hand, developed adverse cardiac remodeling and heart failure.[29] Collectively, these studies strongly suggest that this pathway could be targeted for the treatment of a variety of diseases. Indeed, several biological agents have been successfully developed and approved by FDA by targeting this pathway as treatments for CAPS and this includes IL-1 receptor antagonist anakinra, IL-1β antibody canakinumab, and decoys of IL-1 receptor rilonacept.[18, 30]

Although the pathogenic roles of the NLRP3 inflammasome in a variety of human disorders are quickly emerging, the basis of NLRP3 inflammasome activation and its contribution to disease progression remain not fully understood. It is therefore of importance to develop novel and specific NLRP3 inflammasome inhibitors (NLRP3Is) as pharmacological tools, which will complement

ongoing molecular and genetic studies to precisely define the role of NLRP3 inflammasome in the

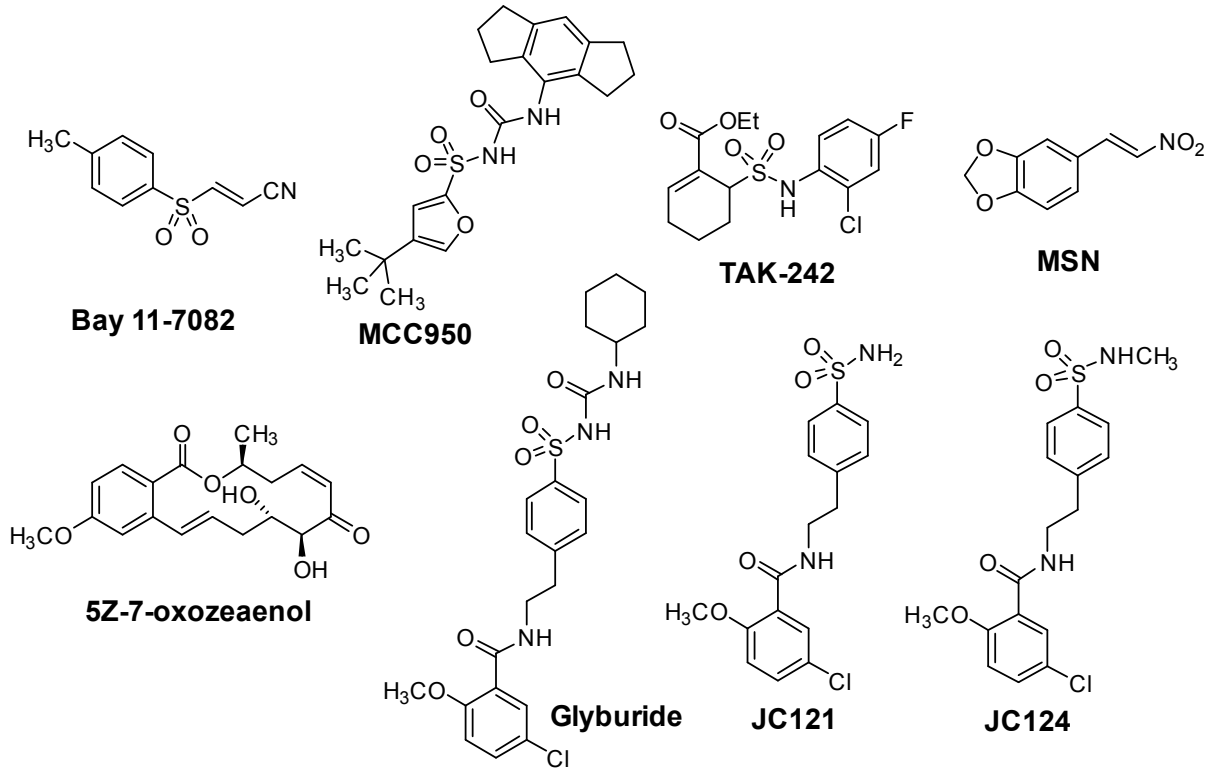


**Figure 1**. Chemical structures of small molecule inhibitors targeting the NLRP3 inflammasome pathway.

pathogenesis of related human diseases, and as potential therapeutics. To this end, several small molecules have recently been reported to inhibit the NLRP3 inflammasome signaling pathway with different or unknown mechanisms of action (MOA) (Figure 1).[31] Among these inhibitors, glyburide is an anti-diabetic drug promoting insulin release and has shown inhibitory activity on NLRP3 inflammasome in myeloid cells *in vitro*.[32] In contrast, glipizide, another sulfonylurea anti-diabetic agent, lacks this inhibitory effect on the NLRP3 inflammasome.[11] This suggests that the observed inhibitory effects on NLRP3 inflammasome by glyburide is independent from its actions on the $K_{ATP}$ channels which are involved in insulin release. Further studies suggested that the sulfonyl and benzamide moieties within this structure are necessary for the observed inhibitory activity.[32] Although the observed anti-inflammatory properties of glyburide suggest beneficial effects, further

development of this compound is limited by the need of high doses that potentially induce lethal hypoglycemia.

Our laboratories have recently designed and developed a sulfonamide analog **JC121** based on the structure of glyburide (Figure 1).[33-35] Biological characterization established that **JC121** is a selective NLRP3I and exhibits promising *in vivo* protective activities in mouse AMI models. Furthermore, as summarized in Figure 2, our studies suggested that **JC121** may directly interfere

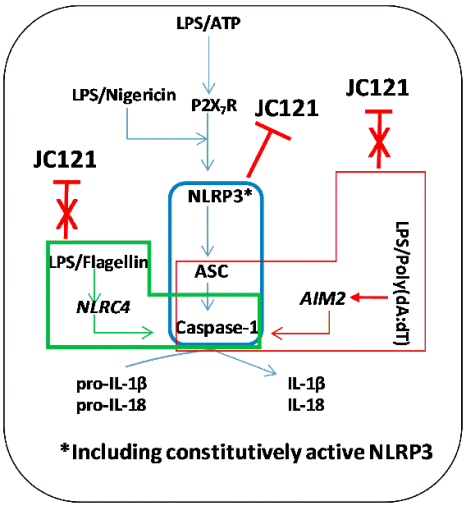


**Figure 2**. Proposed mechanism of action for the benzene sulfonamide analogs as NLRP3Is.

with the formation of the NLRP3 inflammasome complex,[34] based on the facts that 1) it blocks ASC aggregation; 2) it does not directly inhibit caspase-1 activation as NLRC4 and AIM2 pathways are not affected by **JC121**; and 3) it blocks the release of IL-1β and the activation of caspase-1 in macrophages expressing constitutively active NLRP3 from mutant mice. Our ongoing studies also demonstrated the direct binding interactions of our inhibitor with the NLRP3 protein (unpublished data). Based on the structure of **JC121**, we further developed a methylated analog, **JC124**, to balance the hydrophilicity and hydrophobicity (Figure 1). Our initial studies established that **JC124** is an active and selective NLRP3I.[36] Our studies also demonstrated the *in vivo* efficacy of this

compound in reducing AD pathology in a transgenic mouse AD model.[36] Herein, we report further characterization of **JC124** in a transgenic AD mouse model and a mouse AMI mode to confirm its therapeutic effects. Furthermore, structure activity relationship (SAR) studies were conducted to help understand and explore the chemical space of **JC124**, providing guidance for further structural optimization/refinement of this chemical scaffold.

## Results and Discussion

**Therapeutic effects of JC124 on cognitive functions in APP/PS1 mice**. Our previous studies in TgCRND8 mice, a widely used mouse AD model,[37,38] demonstrated that treatment with **JC124** (50 mg/kg) modified multiple AD pathologies, including beta-amyloid (Aβ) deposit, oxidative stress, inflammatory responses, and synaptic degeneration.[36] With the promising activity on AD pathologies, we decided to examine whether such modifications by **JC124** can lead

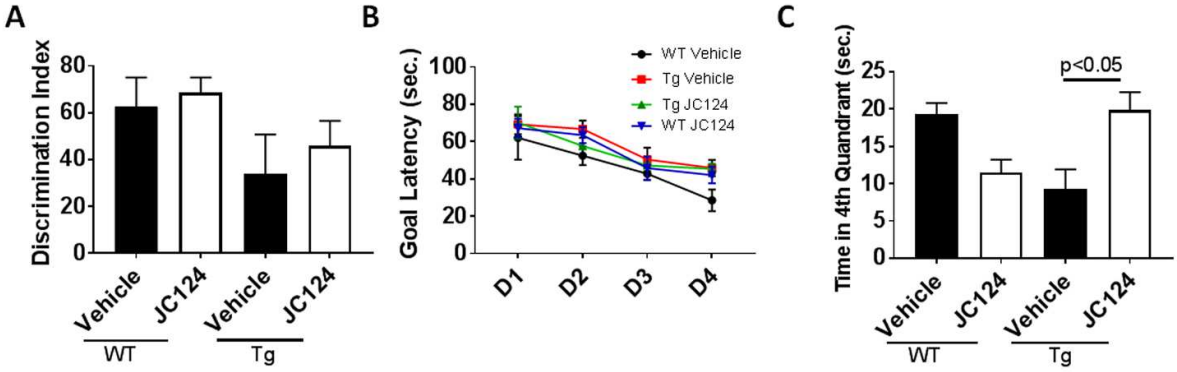


**Figure 3.** Effects of **JC124** treatment on cognitive functions in APP/PS1 mice. At the age of 7 months old, animals were randomly divided into the following experimental groups: WT mice: vehicle group (n=4), JC124 treatment group (n=6). Tg mice: vehicle group (n=5), JC124 treatment group (n=7). Starting at the age of 7 months old, animals were treated for 8 weeks (5 times/week). After completing treatment, animals were tested on cognitive functions using NOR (A) and MWM (B and C) methods.

to improved cognitive functions. We then employed APP/PS1 mice, another widely used mouse AD model,[39] to test **JC124** treatment with a battery of behavioral tests including Novel Object

Recognition (NOR) and Morris Water Maze (MWM). In our previous studies, moderate improvement on AD pathology was observed for **JC124** at a dose of 50 mg/kg,[36] we therefore decided to use a higher dose, 100 mg/kg, in APP/PS1 mice for the behavioral studies. Treatment started at the age of 7 months old and continued for 8 weeks by oral administration (5 times/week). This protocol mimics the therapeutic settings since significant AD pathologies have developed by 7 months old in APP/PS1 mice.[39] As shown in Figure 3A, compared to the wild type (WT) mice, transgenic APP/PS1 (Tg) mice in both vehicle or **JC124** treated groups showed a discrimination index (DI) lower than 50%, which suggested cognitive deficits of Tg mice. **JC124** treatment showed a trend to improve cognitive function with higher DI in **JC124**-treated group compared to the vehicle-treated group. However, the difference did not reach a statistical significance. In MWM fixed-platform test, mice in all groups showed improved learning with time during the 4 days latency trials, however, at the last day of trial, WT vehicle group had shorter latency to find goal platform than the Tg groups, indicating better performance in WT vehicle group in this test (Figure 3B). Notably, in the MWM fixed platform probe trial test, Tg animals treated with **JC124** spent significantly longer time in the goal quadran than the vehicle-treated Tg group, suggesting improved memory function by **JC124** treatment (Figure 3C). A noted, in the MWM probe trial test of WT animals, **JC124** treated mice spent shorter time in the goal quadran compared to the vehicle treated group. Although the difference did not reach stastistical significance, the observed difference may indicate some degree of immune supressive effects by **JC124** treatemnt in normal aniamls that could affect cognitive function. This speculation needs to be confirmed in future study by examining the systemic immune responses. Collectively, under therapeutic trial settings, we

found that **JC124** exhibits beneficial effects on cognition as evidenced by the improved memory function (probe trial).

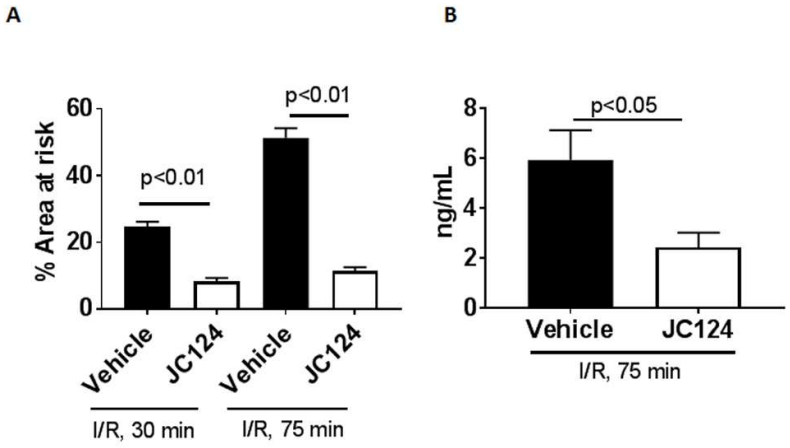


**Figure 4.** Effects of **JC124** in an experimental model of AMI. Mice (n=6 for each group) were subjected to I/R for 30 min or 75 min. Then infarct size (A) was measured by TTC staining and serum troponin I level (B) was determined by ELISA.

**Therapeutic effects of JC124 in an experimental model of AMI.** To further confirm the *in vivo* efficacy of **JC124**, we examined its effects to protect cardiac functions in an experimental AMI model induced by transient myocardial ischemia followed by reperfusion (I/R model), in which the NLRP3 inflammasome has been indicated critical roles on post-ischemia inflammatory responses and heart failure.[25,40] To explore the effective doses of **JC124** and based on the preliminary pharmacokinetic data of **JC124** (unpublished data), we selected a lower dose of 30 mg/kg in this experiment. Two different I/R models were used to evaluate the protective effects of **JC124**: 1) coronary ligation was continued for 30 min; and 2) a more severe model in which coronary ligation was continued for 75 min. As shown in Figure 4, treatment with **JC124** significantly limited the infarct size as measured with triphenyltetrazolium chloride (TTC) staining or troponin I levels in both models when compared to the vehicle treatment group, thus further confirming the *in vivo* efficacy of **JC124** at this dose.

**Design and synthesis of JC124 analogs**. With the confirmation of *in vivo* efficacy, we decided to conduct SAR studies of **JC124** to understand the chemical space around this lead structure. In addition, the results of SAR studies may help shed light on whether this chemical scaffold functions

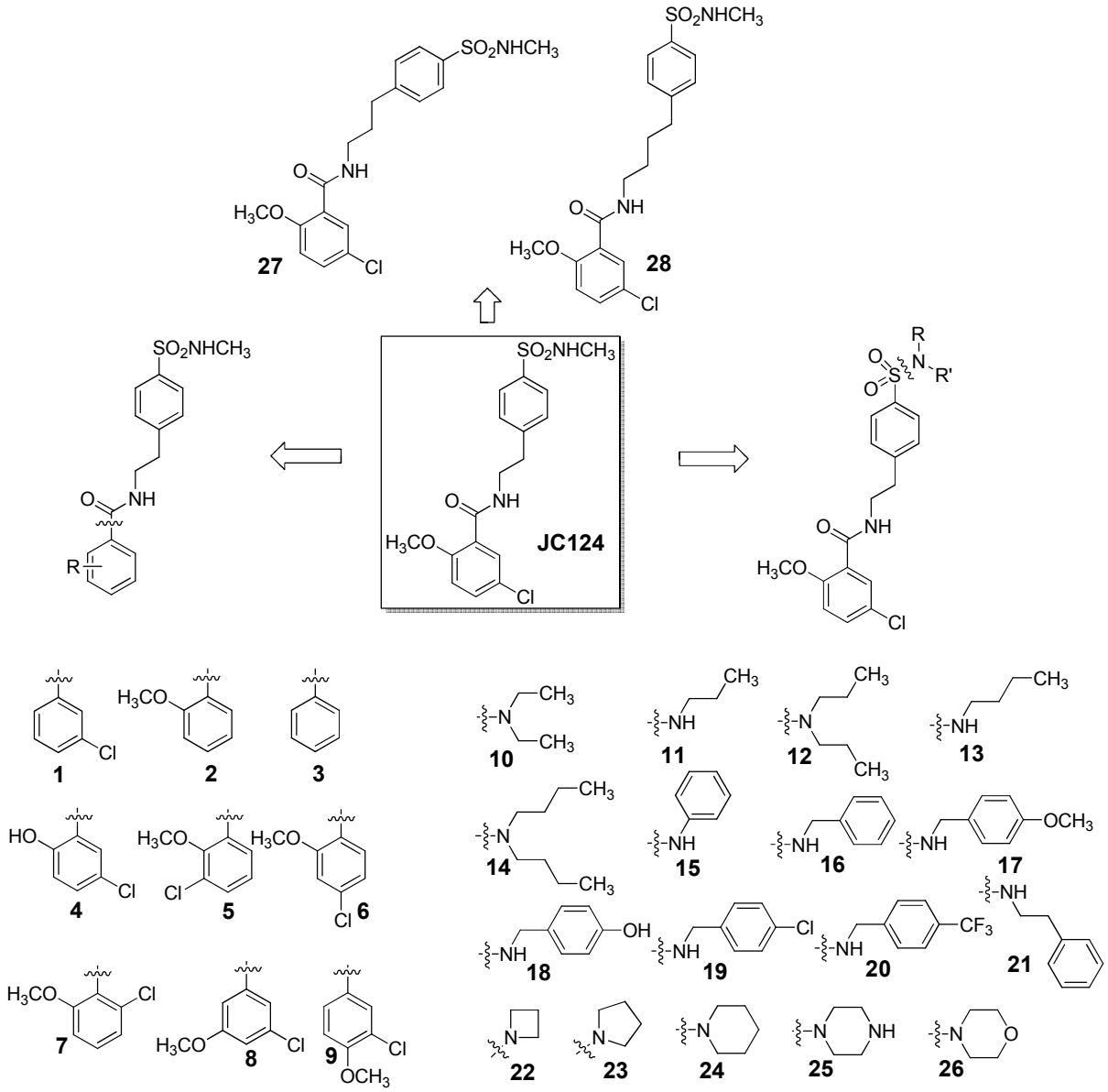


**Figure 5.** Chemical structures of the designed analogs of JC124.

by a single mechanism of action, thus providing valuable information on target interaction. The design of **JC124** congeners was mainly focused on the phenyl domain of the benzamide moiety and

the sulfonamide domain to understand the influence of substituents on their biological activities (Figure 5). Compounds **1-4** were designed to examine the importance of the 2-$CH_3O$ and 5-Cl to their biological activities using the de-construction strategy. Analogs **5-9** were designed to investigate how the positional change of the $CH_3O$- and Cl- substituents will influence their inhibitory activities. The results of **JC124** suggested that the sulfonamide moiety could be optimized to improve biological activity. Therefore, analogs **10-21** were designed to understand the space at this domain for further optimization process. To evaluate whether a cyclized version of sulfonamide analogs will provide improved inhibitory activity, compounds **22-26** were designed. We also designed analogs **27** and **28** to investigate how the linkage length between the two phenyl rings will impact the biological activity.

**Scheme 1**[a]

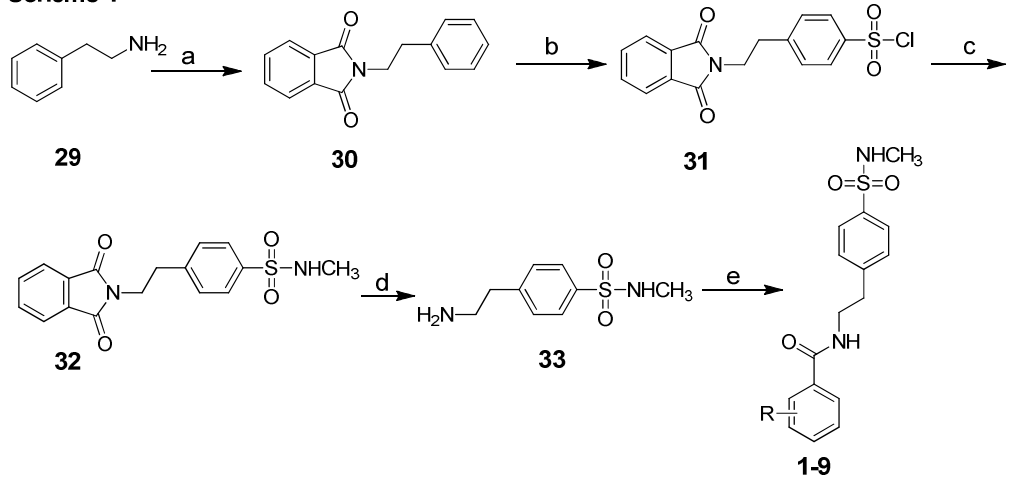


[a]Reagents and conditions. a) phthalic anhydride, AcOH, reflux; b) $ClSO_3H$, 70 °C; c) methylamine, $Et_3N$, DCM, d) $NH_2NH_2$, EtOH, 60 °C; e) various benzoic acids, EDCI, HOBt, $Et_3N$, DCM.

The chemical syntheses of the designed analogs were successfully achieved by employing the conditions detailed in Schemes 1 and 2. Briefly, condensation of 2-phenylethylamine **29** with phthalic anhydride gave **30**, which was on sulfonation with chlorosufonic acid to give intermediate **1**. Reaction of **31** with methylamine afforded intermediate **32**. Refluxing of **32** with $NH_2NH_2$ in

ethanol followed by coupling reactions with corresponding substituted benzoic acids under standard peptide coupling conditions yielded analogs **1-9** (Scheme 1). Compounds **10-26** were synthesized following the conditions listed in Scheme 2. Coupling of **29** with 5-chloro-2-methoxybenzoic acid **34** followed by sulfonation afforded sulfonyl chloride intermediate **36**. Reaction of intermediate **36** with various amines afforded compounds **10-26**. Similarly, compounds **27** and **28** were obtained by following the same strategies with 3-phenylpropylamine **37** or 4-phenylbutylamine **38** as starting material, respectively.

**Scheme 2**[a]

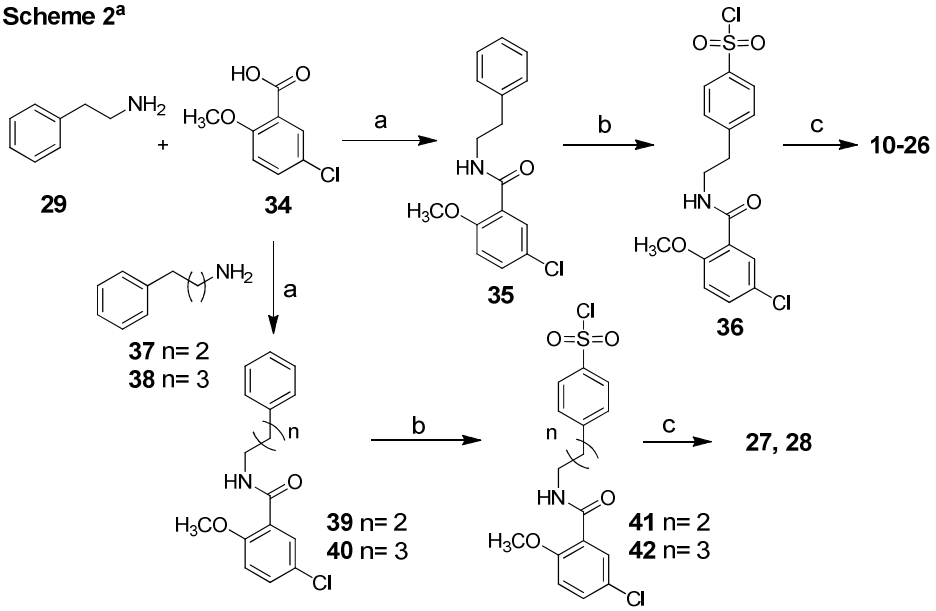


[a]Reagents and conditions. a) EDCI, HOBt, $Et_3N$, DCM; b) $ClSO_3H$, 70 °C; c) various amines, $Et_3N$, DCM.

**Evaluation of the inhibitory potency for the designed analogs on IL-1β release in J774A.1 cells.** Our previous studies have established a cellular model using mouse macrophage J774A.1 cells in which the release of IL-1β is mediated through the activation of NLRP3 inflammasome upon stimulation with lipopolysaccharide (LPS) and adenosine triphosphate (ATP).[33] The level of secreted IL-1β was monitored by an enzyme-linked immunosorbent assay (ELISA). As shown in Table 1, lead compound **JC124** showed an inhibitory potency of 3.25 μM under the current

experimental conditions. Removal of 2-$OCH_3$ or 5-Cl resulted in significant decrease of inhibitory potency (> 4 fold) as demonstrated by analogs **1** and **2**. The importance of the 2-$OCH_3$ and 5-Cl was further demonstrated by analog **3** in which both substituents were removed with a complete loss of inhibitory activity on IL-1β release. When the 2-$OCH_3$ was de-methylated to a 2-OH moiety, a reduced inhibitory potency (~3 fold) was observed in analog **4**. The results of **JC124** and **4** suggest that modification of the 4-OH moiety to other alkoxyl groups at this position could lead to improved inhibitory potency. Move of the 5-Cl to different positions on the phenyl ring all led to significant decrease of inhibitory potency on IL-1β release in J774A.1 cells as evidenced by analogs **5-7**. Interestingly, positional change of the 2-$OCH_3$ to the *meta*-position led to an analog **8** with comparable potency to that of **JC124**, while change to the *para*-position, as demonstrated by **9**, led to significant loss of the inhibitory potency. This may indicate that the electronic effects by the $CH_3O$ substituent is not an essential factor for the observed biological activity. Taken together, the results of **5-9** strongly suggest the important roles of the 2,5-disubstitution on the observed inhibition of IL-1β release under the experimental conditions.

Table 1. Inhibitory potency of the designed analogs on the production of IL-1β by J774A.1 cells upon stimulation with LPS/ATP.

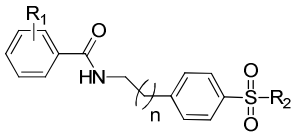


| Compound | $R_1$ | $R_2$ | n= | $IC_{50}$ (μM) |
|---|---|---|---|---|
| **JC124** | 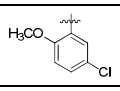 |  | 1 | 3.25 ± 1.34 |
| **1.** |  |  | 1 | 13.36 ± 2.26 |
| **2.** |  |  | 1 | 17.10 ± 4.32 |

| | | | | |
|---|---|---|---|---|
| **3.** |  |  | 1 | 146.56 ± 26.31 |
| **4.** |  |  | 1 | 10.48 ± 0.091 |
| **5.** |  |  | 1 | 31.78 ± 3.19 |
| **6.** |  |  | 1 | 18.031 ± 0.27 |
| **7.** | 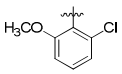 |  | 1 | 44.42 ± 6.32 |
| **8.** | 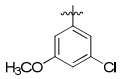 |  | 1 | 5.83 ± 1.36 |
| **9.** | 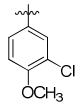 |  | 1 | 32.75 ± 3.78 |
| **10.** | 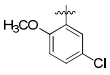 |  | 1 | 2.01 ± 0.43 |
| **11.** | 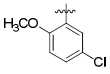 |  | 1 | 1.64 ± 0.20 |
| **12.** | 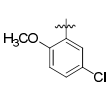 | 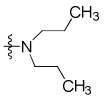 | 1 | 1.40 ± 0.62 |
| **13.** | 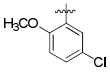 | 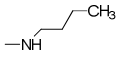 | 1 | 0.97 ± 0.053 |
| **14.** | 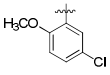 | 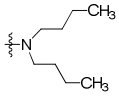 | 1 | 0.55 ± 0.091 |
| **15.** | 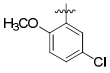 |  | 1 | 2.08 ± 0.59 |
| **16.** | 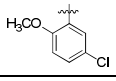 |  | 1 | 1.31 ± 0.16 |
| **17.** | 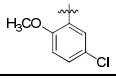 | 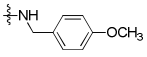 | 1 | 0.42 ± 0.080 |
| **18.** | 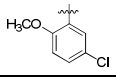 | 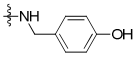 | 1 | 0.63 ± 0.22 |
| **19.** | 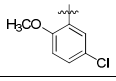 | 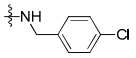 | 1 | 1.50 ± 0.78 |
| **20.** | 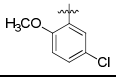 | 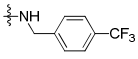 | 1 | 1.90 ± 0.20 |
| **21.** | 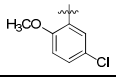 | 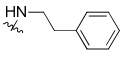 | 1 | 0.81 ± 0.12 |

| | | | | |
|---|---|---|---|---|
| **22.** | 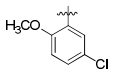 |  | 1 | 1.66 ± 1.21 |
| **23.** | 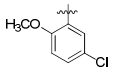 |  | 1 | 3.53 ± 1.68 |
| **24.** | 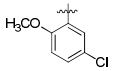 |  | 1 | 5.01 ± 1.33 |
| **25.** | 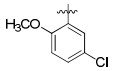 |  | 1 | 3.40 ± 0.62 |
| **26.** | 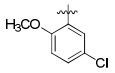 |  | 1 | 3.44 ± 0.97 |
| **27.** | 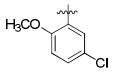 |  | 2 | 2.03 ± 0.61 |
| **28.** | 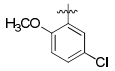 |  | 3 | 1.74 ± 0.61 |

Structural modifications at the sulfonamide moiety, on the other hand, were well tolerated. As shown in Table 1, with the increase of the size of the substituents on the sulfonamide N, the inhibitory potency improves on IL-1β release as reflected by analogs **10-14**. Compound **14** with a di-butyl substitution on the sulfonamide N is the most potent one within this series of analogs with an $IC_{50}$ of 0.55 μM. With this observation, we then turned our attention to more bulky substituents at this position. As shown by **15**, aniline substitution on the sulfonamide moiety resulted in a comparable inhibitory potency to that of **JC124**. Notably, when the benzene ring was replaced with a benzyl moiety as in **16**, the inhibitory potency was increased by 2.5 fold compared to that of **JC124**. Substitution on the benzyl moiety with a 4-$OCH_3$ as illustrated by **17** further improved the inhibitory potency to 0.42 μM, > 3 fold increase compared to that of **16**. Analog **18** with a 4-OH at this position exhibited comparable potency as **17**. This may suggest that an electron-donating group at this specific position favors the inhibitory activity on IL-1β release under the LPS/ATP challenge conditions in J774A.1 cells. This notion is further supported by the results of **19** and **20** as a 4-Cl or 4-$CF_3$ substitution, both electron-withdrawing, led to a comparable or decreased inhibitory potency

to that of **16**. Further structural extension at this position by a phenylethyl moiety, as shown in **21**, resulted in slight improvement when compared to **16**. Analogs with a heterocyclic moiety on the sulfonamide moiety, as demonstrated by compounds **22-26**, exhibited comparable inhibitory potency as that of **JC124**. The results of the mono- or disubstituted analogs suggested that bulky substituents with rotational flexibility are preferred to providing analogs with improved inhibitory potency on IL-1β release. Structural extension slightly improved the inhibitory potency under the current experimental conditions as evidenced by **27** and **28** with an $IC_{50}$ of 2.03 and 1.74 μM, respectively. This is in agreement with the results of compounds **17** and **21**, thus suggesting that hydrophobic interactions at this domain may be important for the observed inhibition on IL-1β release.

**Compounds 14 and 17 are selective NLRP3Is.** After the establishment of inhibitory potency on IL-1β release in J774A.1 cells for the designed analogs, we selected **14** and **17**, the two most potent analogs, for further characterization in mouse bone marrow derived macrophages (BMDMs) and in mice. As shown in Figures 6A, both **14** and **17** dose dependently suppressed the release of IL-1β from BMDMs upon LPS/ATP challenge with an $IC_{50}$ of 0.12 ± 0.067 and 0.36 ± 0.043 μM, respectively. Analog **14** is ~4 times more potent in BMDMs than in J774A.1 cells to inhibit the release

of IL-1β, while the potency of **17** is comparable in these two cell populations. This may suggest that BMDMs are more sensitive to **14** under the current experimental conditions, consistent with our previous studies.[41] We next examined the selectivity of **14** and **17** to NLRP3 inflammasome. To this end, J774A.1 cells were stimulated with LPS/poly(dA:dT) or LPS/flagellin to activate the NLRC4 and AIM2 inflammasome, respectively. As shown in Figures 6B and 6C, treatment of J774A.1 cells

with **14** or **17** under these experimental conditions did not significantly interfere with the production of IL-1β (by ANOVA one-way analysis), thus confirming the relatively specific inhibition of NLRP3 inflammasome by **14** and **17**. Consistent with the reported results,[36,42] no inhibitory activity was observed for **JC124** and **MCC950**, a recently reported and potent inhibitor that targets the NLRP3 inflammasome pathway,[42] under these conditions as well. The results from the selectivity

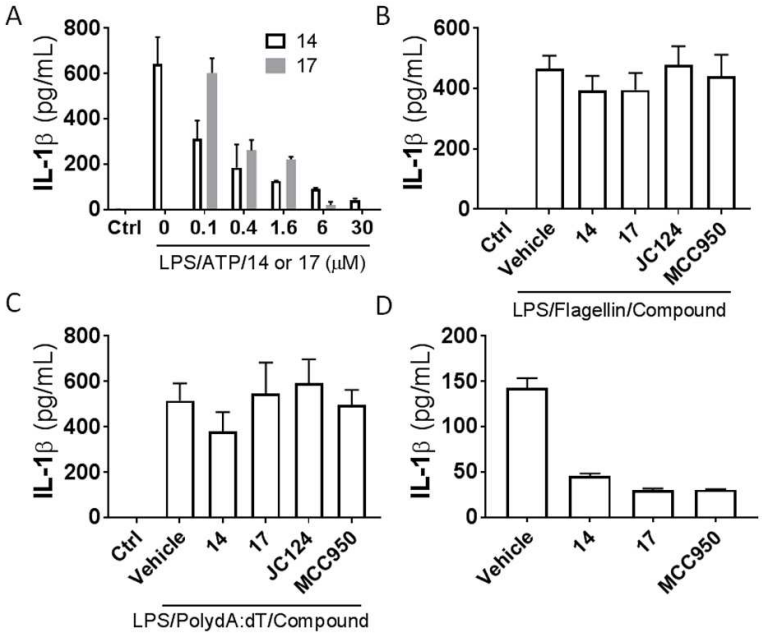


**Figure 6.** Compounds **14** and **17** blocks NLRP3 inflammasome activation and IL-1β production in primary macrophages and LPS-challenged mice. (A) BMDMs were primed with LPS (1 μg/mL) for 4.5 h and then treated with indicated doses of 14 or 17 when adding ATP (5 mM) stimulation for 30 min. IL-β in the culture media was assayed by ELISA. (B and C) J774A.1 cells were treated with LPS (1 μg/mL) and test compounds (10 μM) for 1 h. Flagellin (1 μg/mL) was added and allowed to incubate for 6 hr or (Poly(dA:dT)) (4 μg/ml) for 8 hr. The supernatants were collected and levels of IL-1β were measured by ELISA. (D) Serum levels of IL-1β from C57BL/6 mice pretreated with 14 and 17 (0.5 mg/kg) or vehicle control were measured by ELISA 2.5 h after i.p. injection of LPS (20 mg/kg)

studies also serve as an indirect evidence to support the MOA that analogs derived from this chemical scaffold interfere with the NLRP3 inflammasome complex, instead of the upstream priming step by the LPS. This is consistent with our previously reported results.[34] Finally, we tested

the *in vivo* engagement of the NLRP3 inflammasome by **14** and **17**. Mice were pretreated with **14** or **17** before intraperitoneal injection of LPS, which has been shown to trigger IL-1β production in a NLRP3-dependent manner.[43] **MCC950** was tested as a positive control. As shown in Figure 6D, serum levels of IL-1β was sharply reduced by the treatment of all three compounds at the tested dose, thus strongly suggesting the engagement of the NLRP3 inflammasome pathway in the observed effects by **14** and **17**. Although compounds **14** and **17** exhibit significantly improved potency when compared to **JC124**, they are still less potent than MCC950. However, compounds **14** and **17** exhibited comparable activity to MCC950 in this *in vivo* LPS-challenge experiment. This could be caused by different pharmacokinetic properties of these analogs as well as the unique MOA of our inhibitors. Further studies are warranted to investigate and confirm these speculations.

**Conclusion**

In our efforts to develop small molecule inhibitors by targeting the NLRP3 inflammasome, a sulfonamide based chemical scaffold was identied to provide analogs as active NLRP3Is. In this study, we further confirmed the *in vivo* activity of **JC124**, a recently identified lead inhibitor from our group, in a transgenic AD mouse model and a mouse AMI model. The results clearly provided confidence for further develop of new analogs based on this chemcial scaffold. Further SAR studies revealed the positions on the structure of **JC124** for further optimization. Our results demonstrated that the 2-$OCH_3$ and 5-Cl are essential to the inhibitory activity on the NLRP3 inflammasome as positional change or removal of them led to significant decrease of inhibitory activity. On the other hand, structural modifications on the N-substituents of the sulfonamide moiety are tolerated and bulky groups tend to provide analogs with improved potency. As a result of this SAR study, two new lead compounds, **14** and **17**, were identified with improved inhibitory potency. Further

biological characterization in BMDMs and J774A.1 cells confirmed the inhibitory potency and selectivity of these two lead compounds to the NLRP3 inflammasome. More importantly, studies in LPS-challenged mice, a mouse model in which the release of IL-1β is NLRP3 inflammasome dependent, confirmed that both **14** and **17** signifiantly suppressed the production of IL-1β, thus confirming the *in vivo* engagement of this inflammasome complex by these two compounds. Collectively, the results strongly encourage further studies and development of new analogs based on this chemical scaffold as NLRP3Is and explore their potential therapeutic applications.

**Experimental Section**

**Chemistry.** Reagents and solvents were obtained from commercial suppliers and used as received unless otherwise indicated. All reactions were carried out under inert atmosphere ($N_2$) unless otherwise noted. Reactions were monitored by thin-layer chromatography (TLC) (precoated silica gel 60 $F_{254}$ plates, EMD Chemicals) and visualized with UV light or by treatment with Phosphomolybdic acid (PMA). Flash chromatography was performed on silica gel (200-300 mesh, Fisher Scientific) using solvents as indicated. $^{1}$HNMR and $^{13}$CNMR spectra were routinely recorded on Bruker ARX 400 spectrometer. The NMR solvent used was $CDCl_3$ or DMSO-$d_6$ as indicated. Tetramethylsilane (TMS) was used as internal standard. The purity of target NLRPIs was determined by HPLC using Varian 100-5 C18 250 x 4.6 mm column with UV detection (288 nm) (50% acetonitrile/50% $H_2O$/0.1 % trifluoroacetic acid (TFA) and 80% methanol/19.9% $H_2O$/0.1% TFA two solvent systems) to be ≥ 95%.

**3-chloro-*N*-(4-(*N*-methylsulfamoyl)phenethyl)benzamide (1).** Compound **1** was prepared from 3-Chlorobenzoic acid (0.47 mmol) following Method C in 91% yield. $^{1}$H NMR (400 MHz, DMSO-$d_6$) δ 8.69 (t, *J*= 5.44 Hz, 1H), 7.83 (t, *J* = 1.76 Hz, 1H), 7.76 (dt, *J* = 7.80, 1.35 Hz, 1H),

7.70 (d, *J* = 8.28 Hz, 2H), 7.61- 7.59 (m, 1H), 7.52 - 7.46 (m, 4H), 3.53 (q, *J* = 6.64 Hz, 2H), 2.95 (t, *J* = 7.16 Hz, 2H), 2.39 (d, *J* = 5.04 Hz, 3H); $^{13}$C NMR (100 MHz, DMSO-$d_6$) δ 164.8, 144.3, 137.2, 136.5, 133.1, 130.9, 130.8, 129.4, 126.9, 126.7, 125.8, 40.4, 34.6, 28.6.

**2-methoxy-*N*-(4-(*N*-methylsulfamoyl)phenethyl)benzamide (2)** Compound **2** was prepared from 2-methoxybenzoic acid (0.47 mmol) following Method C in 65% yield. $^{1}$H NMR (400 MHz, DMSO-$d_6$) δ 8.18 (t, *J*= 5.58 Hz, 1H), 7.70 - 7.74 (m, 3H), 7.50 (d, *J* = 8.38 Hz, 2H), 7.45 (dt, *J* = 2.01, 7.91 Hz 1H), 7.38 (q, *J* = 5.03 Hz, 1H), 7.11 (d, *J* = 8.20 Hz, 1H), 7.02 (dt, *J* = 7.57, 0.78 Hz, 1H), 3.81 (s, 3H), 3.57 (q, *J* = 6.60 Hz, 2H), 2.94 (t, *J* = 7.02 Hz, 2H), 2.41 (d, *J* = 5.04 Hz, 3H); $^{13}$C NMR (100 MHz, DMSO-$d_6$) δ 164.9, 156.9 144.4, 137.2, 132.1, 130.3, 129.5, 126.7, 123.0, 120.0, 111.9, 55.8, 40.1, 34.7, 28.6.

***N*-(4-(*N*-methylsulfamoyl)phenethyl)benzamide (3)** Compound **3** was prepared starting from benzoic acid (0.47 mmol) following Method C in 56% yield. $^{1}$H NMR (400 MHz, DMSO-$d_6$) δ 8.61 (t, *J* = 5.46 Hz, 1H), 7.85 (d, *J* = 8.00 Hz, 2H), 7.75 (d, *J* = 8.00 Hz, 2H), 7.59 - 7.48 (m, 5H), 7.41 (q, *J* = 5.01 Hz, 1H), 3.59 (q, *J* = 6.68 Hz, 2H), 3.00 (t, *J* = 7.20 Hz, 2H), 2.44 (d, *J* = 5.04 Hz, 3H); $^{13}$C NMR (100 MHz, DMSO-$d_6$) δ 164.2, 144.5, 137.1, 134.5, 131.0, 129.4, 128.2, 127.0, 126.7, 40.3, 34.8, 28.6.

**5-chloro-2-hydroxy-*N*-(4-(*N*-methylsulfamoyl)phenethyl)benzamide (4).** Compound **4** was prepared from 5-chlorosalicylic acid (0.47 mmol) following Method C in 60% yield. $^{1}$H NMR (400 MHz, DMSO-$d_6$) δ 8.94 (t, *J*= 5.46 Hz, 1H), 7.71 (d, *J* = 8.28 Hz, 2H), 7.48 (d, *J* = 8.28 Hz, 2H), 7.42 (dd, *J* = 9.03, 2.69 Hz, 1H), 7.37 (q, *J* = 5.03 Hz, 1H), 6.93 (d, *J* = 8.84 Hz, 1H), 3.58 (q, *J* = 6.64 Hz, 2H), 2.96 (t, *J* = 7.14 Hz, 2H), 2.39 (d, *J* = 5.04 Hz, 3H); $^{13}$C NMR (100 MHz,

DMSO-$d_6$) δ 167.4 , 158.4 144.1, 137.2, 133.2, 129.4, 127.3, 126.8, 122.9, 119.3, 116.9, 40.1, 34.5, 28.6.

**3-chloro-2-methoxy-*N*-(4-(*N*-methylsulfamoyl)phenethyl)benzamide (5).** Compound **5** was prepared from 3-chloro-2-methoxybenzoic acid (0.27 mmol) following Method C in 40% yield. $^1$H NMR (400 MHz, DMSO-$d_6$) δ 8.46 (t, $J$ = 5.48 Hz, 1H), 7.77 (d, $J$ = 8.24 Hz, 2H), 7.62 (dd, $J$ = 8.16, 1.53 Hz, 1H), 7.56 (d, $J$ = 8.24 Hz, 2H), 7.44 - 7.40 (m, 2H), 7.24 (t, $J$ = 7.84 Hz, 1H), 3.73 (s, 3H), 3.61 (q, $J$ = 6.59 Hz, 2H), 3.01 (t, $J$ = 7.04 Hz, 2H), 2.46 (d, $J$ = 5.04 Hz, 3H); $^{13}$C NMR (100 MHz, DMSO-$d_6$) δ 165.1, 152.8, 144.3, 137.2, 132.1, 131.7, 129.4, 128.2, 127.1, 126.7, 125.0, 61.5, 34.5, 28.6.

**4-chloro-2-methoxy-*N*-(4-((methylamino)sulfinyl)phenethyl)benzamide (6).** Compound **6** was prepared from 4-chloro-2-methoxybenzoic acid (0.54 mmol) following Method C in 60% yield. $^1$H NMR (400 MHz, DMSO-$d_6$) δ 8.22 (t, $J$ = 5.58 Hz, 1H), 7.77 (d, $J$ = 8.33 Hz, 2H), 7.74 (d, $J$ = 8.32 Hz, 1H), 7.53 (d, $J$ = 8.32 Hz, 2H), 7.42 (q, $J$ = 4.84 Hz, 1H), 7.25 (d, $J$ = 1.88 Hz, 1H), 7.13 (dd, $J$ = 8.34, 1.95 Hz, 1H), 3.88 (s, 3H), 3.60 (q, $J$ = 6.95 Hz, 2H), 2.98 (t, $J$ = 6.97 Hz, 2H), 2.45 (d, $J$ = 4.88 Hz, 3H); $^{13}$C NMR (100 MHz, DMSO-$d_6$) δ 164.0, 157.6, 144.4, 137.2, 136.3, 131.7, 129.4, 126.7, 122.1, 120.5, 112.5, 56.3, 40.1, 34.7 28.6.

**2-chloro-6-methoxy-N-(4-((methylamino)sulfinyl)phenethyl)benzamide (7).** Compound **7** was prepared from 2-Chloro-6-methoxybenzoic acid (0.54 mmol) following Method C in 62% yield. $^1$H NMR (400 MHz, DMSO-$d_6$) δ 8.49 (t, $J$ = 5.05 Hz, 1H), 7.70 (d, $J$ = 8.32 Hz, 2H), 7.50 (d, $J$ = 8.32 Hz, 2H), 7.39 - 7.31 (m, 2H), 7.04 - 7.01 (m, 2H), 3.75 (s, 3H), 3.49 (q, $J$ = 7.01 Hz, 2H), 2.91 (t, $J$ = 7.01 Hz, 2H) 2.41 (d, $J$ = 5.04 Hz, 3H); $^{13}$C NMR (100 MHz, DMSO-$d_6$) δ 163.9, 156.9, 144.3, 137.1, 130.4, 129.5, 127.2, 126.6, 120.9, 110.3, 56.0, 34.5, 28.6.

**3-chloro-5-methoxy-*N*-(4-(*N*-methylsulfamoyl)phenethyl)benzamide (8).** Compound **8** was prepared from 3-chloro-5-methoxybenzoic acid (0.36 mmol) following Method C in 70% yield. $^1$H NMR (400 MHz, DMSO-$d_6$) δ 8.66 (t, $J$ = 5.48 Hz, 1H), 7.70 (d, $J$ = 8.33 Hz, 2H), 7.46 (d, $J$ = 8.33 Hz, 2H), 7.42 - 7.41 (m, 1H), 7.36 (q, $J$ = 5.03 Hz, 1H), 7.34 - 7.32 (m, 1H), 7.19 - 7.18 (m, 1H), 3.82 (s, 3H), 3.53 (q, $J$ = 6.64 Hz, 2H), 2.94 (t, $J$ = 7.14 Hz, 2H), 2.40 (d, $J$ = 5.04 Hz, 3H); $^{13}$C NMR (100 MHz, DMSO-$d_6$) δ 164.6, 160.1, 144.3, 137.3, 137.2, 133.8, 129.4, 126.7, 119.1, 111.9, 55.81, 40.4, 34.6, 28.6.

**3-chloro-4-methoxy-*N*-(4-(*N*-methylsulfamoyl)phenethyl)benzamide (9).** Compound **9** was prepared from 3-chloro-4-methoxybenzoic acid (0.36 mmol) following Method C in 70% yield. $^1$H NMR (400 MHz, DMSO-$d_6$) δ 8.59 (t, $J$ = 5.46 Hz, 1H), 7.94 (d, $J$ = 2.24 Hz, 1H), 7.85 (dd, $J$ = 2.24, 8.71 Hz, 1H), 7.75 (d, $J$ = 8.29 Hz, 2H), 7.51 (d, $J$ = 8.28 Hz, 2H), 7.40 (q, $J$ = 5.06 Hz, 1H), 7.27 (d, $J$ = 8.72 Hz, 1H), 3.96 (s, 3H), 3.56 (q, $J$ = 7.06 Hz, 2H), 2.98 (t, $J$ = 7.06 Hz, 2H), 2.44 (d, $J$ = 5.06 Hz, 3H); $^{13}$C NMR (100 MHz, DMSO-$d_6$) δ 164.5, 156.7, 144.4, 137.2, 129.4, 128.7, 127.7, 127.5, 126.7, 120.8, 112.3, 56.4, 40.3, 34.8, 28.6.

**5-chloro-*N*-(4-(*N*,*N*-diethylsulfamoyl)phenethyl)-2-methoxybenzamide** (**10**). Compound **10** was prepared from **36** (0.39 mmol) and diethylamine (1.95 mmol) following Method B in 87% yield. $^1$H NMR (400 MHz, DMSO-$d_6$) δ 8.26 (t, $J$ = 5.77 Hz, 1H), 7.73 (d, $J$ = 8.38 Hz, 1H), 7.60 (d, $J$ = 2.70 Hz, 1H), 7.51 - 7.46 (m, 3H), 7.16 (d, $J$ = 9.54 Hz, 1H), 3.81 (s, 3H), 3.57 (q, $J$ = 6.93 Hz, 2H), 3.96 (q, $J$ = 7.60 Hz, 4H), 2.95 (t, $J$ = 7.60 Hz, 2H), 1.04 (t, $J$ = 7.25 Hz, 6H); $^{13}$C NMR (100 MHz, DMSO-$d_6$) δ 163.6, 155.7, 144.5, 137.7, 137.4, 129.6, 129.5, 129.7, 124.8, 124.3, 114.2, 56.2, 41.7, 40.1, 34.6, 14.0.

**5-chloro-2-methoxy-*N*-(4-(*N*-propylsulfamoyl)phenethyl)benzamide (11).** Compound **11** was prepared from **36** (0.39 mmol) and propylamine (1.95 mmol) following method B in 61% yield. $^{1}$H NMR (400 MHz, DMSO-$d_6$) δ 8.24 (t, $J$ = 3.50 Hz, 1H), 7.72 (d, $J$ = 8.20 Hz, 2H), 7.61 (d, $J$ = 2.08 Hz, 1H), 7.51 - 7.46 (m, 3H), 7.15 (d, $J$ = 8.88 Hz, 1H), 3.81 (s, 3H), 3.55 (q, $J$ = 6.60 Hz, 2H), 2.92 (t, $J$ = 7.02 Hz, 2H), 2.67 (q, $J$ = 6.68 Hz, 2H), 1.36 (sex, $J$ = 7.16 Hz, 2H), 0.77 (t, $J$ = 7.38 Hz, 3H); $^{13}$C NMR (100 MHz, DMSO-$d_6$) δ 163.6, 155.7, 144.1, 138.6, 131.5, 129.6, 129.4, 126.5, 124.9, 124.3, 114.2, 56.2, 44.3, 40.1, 34.6, 22.3, 11.1.

**5-chloro-*N*-(4-(*N*,*N*-dipropylsulfamoyl)phenethyl)-2-methoxybenzamide (12).** Compound **12** was prepared from **36** (0.39 mmol) and dipropylamine (1.95 mmol) following following Method B in 75% yield. $^{1}$H NMR (400 MHz, DMSO-$d_6$) δ 8.24 (t, $J$ = 5.50 Hz, 1H), 7.72 ( d, $J$ = 8.28 Hz, 2H), 7.61 (d, $J$ = 2.80 Hz, 1H), 7.51 - 7.47 (m, 3H), 7.15 (d, $J$ = 8.88 Hz, 1H), 3.83 (s, 3H), 3.56 (q, $J$ = 6.58 Hz, 2H), 3.00 (t, $J$ = 7.54 Hz, 4H), 2.94 (t, $J$ = 6.96 Hz, 2H), 1.46 (sex, $J$ = 7.47 Hz, 4H), 0.80 (t, $J$ = 7.38 Hz, 6H); $^{13}$C NMR (100 MHz, DMSO-$d_6$) δ 163.6, 155.7, 144.5, 137.4, 131.4, 129.6, 129.5, 126.8, 124.8, 124.3, 114.2, 56.3, 49.7, 40.1, 34.6, 21.6, 10.9.

***N*-(4-(*N*-butylsulfamoyl)phenethyl)-5-chloro-2-methoxybenzamide (13).** Compound **13** was prepared from **36** (0.39 mmol) and butylamine (1.95 mmol) following following method B in 56% yield. $^{1}$H NMR (400 MHz, DMSO-$d_6$) δ 8.25 (t, $J$ = 5.58 Hz, 1H), 7.73 (d, $J$ = 8.32 Hz, 2H), 7.62 (d, $J$ = 2.80 Hz, 1H), 7.51 - 7.47 (m, 3H), 7.15 (d, $J$ = 8.92 Hz, 1H), 3.82 (s, 3H), 3.55 (q, $J$ = 6.60 Hz, 2H), 2.93 (t, $J$ = 7.00 Hz, 2H), 2.71 (q, $J$ = 6.60 Hz, 2H), 1.37 - 1.17 (m, 4H), 0.78 (t, $J$ = 7.28 Hz, 3H); $^{13}$C NMR (100 MHz, DMSO-d$_6$) δ 163.6, 155.7, 144.1, 138.5, 131.4, 129.5, 129.4, 126.5, 124.9, 124.3, 114.2, 56.2, 42.2, 40.2, 34.6, 31.0, 19.4, 13.4.

**5-chloro-*N*-(4-(*N*,*N*-dibutylsulfamoyl)phenethyl)-2-methoxybenzamide (14).** Compound **14** was prepared from compound **36** (0.39 mmol) and dibutylamine (1.95 mmol) following method B in 86% yield. (400 MHz, DMSO-$d_6$) δ 8.26 (t, $J$ = 5.42 Hz, 1H), 7.71 (d, $J$ = 8.32 Hz, 2H), 7.63 (d, $J$ = 2.80 Hz, 1H), 7.51 - 7.47 (m, 3H), 7.15 (d, $J$ = 8.92 Hz, 1H), 3.82 (s, 3H), 3.54 (q, $J$ = 6.53 Hz, 2H), 3.02 (t, $J$ = 7.52 Hz, 4H), 2.93 (t, $J$ = 7.00 Hz, 2H), 1.41 (qun, $J$ = 7.52 Hz, 4H), 1.22 (sex, $J$ = 7.40 Hz, 4H), .837 (t, $J$ = 7.34 Hz, 6H); $^{13}$C NMR (100 MHz, DMSO-$d_6$) δ 163.6, 155.7, 144.1, 138.5, 131.4, 129.5, 129.4, 126.5, 124.9, 124.3, 114.2, 56.2, 42.2, 40.2, 34.6, 31.0, 19.2, 13.5.

**5-chloro-2-methoxy-*N*-(4-(*N*-phenylsulfamoyl)phenethyl)benzamide (15).** Compound **15** was prepared from compound **36** (0.26 mmol) and aniline (1.30 mmol) following method B in 80% yield. Purity was confirmed by HPLC: $^1$H NMR (400 MHz, DMSO-$d_6$) δ 8.25 (t, $J$ = 5.56 Hz, 1H), 7.70 (d, $J$ = 8.36 Hz, 2H), 7.61 (d, $J$ = 2.80 Hz, 1H), 7.49 (dd, $J$ = 8.88, 2.89 Hz, 1H), 7.42 (d, $J$ = 8.36 Hz, 2H), 7.19 (d, $J$ = 2.78 Hz, 2H), 7.13 (d, $J$ = 8.92 Hz, 1H), 7.09 (d, $J$ = 4.34 Hz, 2H), 7.00 (t, $J$ = 7.64 Hz, 1H), 3.73 (s, 3H), 3.50 (q, $J$ = 6.56 Hz, 2H), 2.87 (t, $J$ = 7.02 Hz, 3H); $^{13}$C NMR (100 MHz, DMSO-$d_6$) δ 163.6, 155.6, 144.8, 137.7, 137.5, 131.4, 129.5, 129.4, 129.1, 126.7, 124.8, 124.3, 123.9, 119.9, 114.1, 56.1, 34.5, 30.6.

***N*-(4-(*N*-benzylsulfamoyl)phenethyl)-5-chloro-2-methoxybenzamide (16).** Compound **16** was prepared from compound **36** (1.28 mmol) and benzylamine (6.40 mmol) following method B in 72% yield. $^1$H NMR (400 MHz, DMSO-$d_6$) δ 8.27 (t, $J$ = 5.56 Hz, 1H), 8.09 (t, $J$ = 5.90 Hz, 1H), 7.76 (d, $J$ = 8.32 Hz, 2H), 7.65 (d, $J$ = 2.08 Hz, 1H) 7.50 (dd, $J$ = 9.05, 3.15 Hz, 1H), 7.47 (d, $J$ = 8.32 Hz, 2H), 7.29 - 7.19 (m, 3H), 7.16 (d, $J$ = 8.92 Hz, 1H), 3.97 (d, $J$ = 5.60 Hz, 2H), 3.83 (s, 3H), 3.56 (q, $J$ = 6.62 Hz, 2H), 2.93 (t, $J$ = 7.06 Hz, 2H); $^{13}$C NMR (100 MHz, DMSO-$d_6$) δ 163.6,

155.7, 144.2, 138.7, 137.6, 131.5, 129.5, 129.4, 128.2, 127.5, 127.1, 126.6, 124.9, 124.4, 114.2, 56.3, 46.1, 40.2, 34.6.

**5-chloro-2-methoxy-N-(4-(N-(4-methoxybenzyl)sulfamoyl)phenethyl)benzamide (17).** Compound **17** was prepared from compound **36** (0.26 mmol) and 4-methoxybenzylamine (1.30 mmol) following method B in 69% yield. $^{1}$H NMR (400 MHz, DMSO-$d_6$) δ 8.28 (t, J = 5.46 Hz, 1H), 8.00 (t, J = 6.22 Hz, 1H), 7.75 (d, J = 8.12 Hz, 2H), 7.64 (d, J = 2.68 Hz, 1H), 7.51 (dd, *J* = 8.99, 2.39 Hz, 1H), 7.46 (d, J = 8.20 Hz, 2H), 7.17 (d, J = 8.92 Hz, 1H), 7.13 (d, J = 8.56 Hz, 2H), 6.83 (d, J = 8.60 Hz, 2H), 3.90 (d, J = 6.20 Hz, 2H), 3.83 (s, 3H), 3.72 (s, 3H), 3.56 (q, J = 6.55 Hz, 2H), 2.94 (t, J = 7.04 Hz, 2H); $^{13}$C NMR (100 MHz, DMSO-$d_6$) δ 163.6, 158.4, 155.7, 144.2, 138.7, 131.5, 129.5, 129.4, 128.9, 126.6, 126.7, 124.9, 124.3, 114.2, 113.6, 56.3, 55.03, 45.7, 40.2, 34.7.

**5-chloro-*N*-(4-(*N*-(4-hydroxybenzyl)sulfamoyl)phenethyl)-2-methoxybenzamide (18).** Compound **18** was prepared from compound **36** (0.39 mmol) and 4-(aminomethyl)phenol (1.95 mmol) following method B in 51% yield. $^{1}$H NMR (400 MHz, DMSO-$d_6$) δ 9.30 (br. s., 1H), 8.28 (t, *J* = 5.46 Hz, 1H), 7.92 (t, *J* = 6.20 Hz, 1H), 7.74 (d, *J* = 8.20 Hz, 2H), 7.64 (d, *J* = 2.80 Hz, 1H), 7.50 (dd, *J* = 8.96, 2.89 Hz, 1H), 7.46 (d, *J* = 8.24 Hz, 2H), 7.16 (d, *J* = 8.92 Hz, 1H), 7.00 (d, *J* = 8.04 Hz, 2H), 6.65 (d, *J* = 8.44 Hz, 2H), 3.83 - 3.82 (m, 5H), 3.55 (q, *J* = 6.60 Hz, 2H), 2.93 (t, *J* = 7.02 Hz, 2H); $^{13}$C NMR (100 MHz, DMSO-$d_6$) δ 163.6, 156.5, 155.7, 144.2, 138.7, 131.5, 129.5, 129.4, 128.4, 127.6, 124.9, 124.3, 114.9 114.2, 56.4, 56.3, 45.8 40.3, 34.7.

**5-chloro-*N*-(4-(*N*-(4-chlorobenzyl)sulfamoyl)phenethyl)-2-methoxybenzamide** (**19**). Compound **19** was prepared from compound **36** (0.39 mmol) and 4-chlorobenzylamine (1.95 mmol) following method B in 45% yield. $^{1}$H NMR (400 MHz, DMSO-$d_6$) δ 8.28 (t, *J* = 5.58 Hz, 1H), 8.14 (t, *J* = 6.26 Hz, 1H), 7.74 (d, *J* = 8.32 Hz, 2H), 7.64 (d, *J* = 2.80 Hz, 1H), 7.50 (dd, *J* = 8.79,

2.77 Hz, 1H), 7.46 (d, *J* = 8.28 Hz, 2H), 7.32 (d, *J* = 8.56 Hz, 2H), 7.24 (d, *J* = 8.56 Hz, 2H), 7.16 (d, *J* = 8.92 Hz, 1H), 3.97 (d, *J* = 6.12 Hz, 2H), 3.82 (s, 3H), 3.55 (q, *J* = 6.63 Hz, 2H), 2.93 (t, *J* = 7.08 Hz, 2H); $^{13}$C NMR (100 MHz, DMSO-$d_6$) δ 163.6, 155.7, 144.3, 138.6, 136.8, 131.7, 131.5, 129.6, 129.5, 129.4, 128.1, 126.5, 124.9, 124.3, 114.2, 56.2, 45.3 40.2, 34.7.

**5-chloro-*N*-(4-(*N*-(4-(trifluoromethyl)benzyl)sulfamoyl)phenethyl)-2-methoxybenzamide** (**20**). Compound **20** was prepared from compound **36** (0.39 mmol) and 4-(trifluoromethyl)benzyl−amine (1.95 mmol) following method B in 48% yield. $^{1}$H NMR (400 MHz, DMSO-$d_6$) δ 8.23-8.27 (m, 2H), 7.74 (d, *J* = 7.88 Hz, 2H), 7.62-7.64 (m, 3H), 7.51 (d, *J* = 8.88 Hz, 1H), 7.44-7.46 (m, 4H), 7.17 (d, *J* = 8.84 Hz, 1H), 4.09 (d, *J* = 5.92 Hz, 2H), 3.82 (s, 3H), 3.56 (q, *J* = 6.24 Hz, 2H), 2.93 (t, *J* = 6.80 Hz, 2H); $^{13}$C NMR (100 MHz, DMSO-$d_6$) δ 163.6, 155.7, 144.3, 142.6, 138.5, 131.4, 129.4, 128.1, 126.5, 125.0, 124.9, 124.8, 124.3, 114.1, 56.2, 45.5, 40.2, 34.6.

**5-chloro-2-methoxy-*N*-(4-(*N*-phenethylsulfamoyl)phenethyl)benzamide** (**21**). Compound **21** was prepared from compound **36** (0.32 mmol) and phenylethylamine (1.60 mmol) following method B in 69% yield. $^{1}$H NMR (400 MHz, DMSO-$d_6$) δ 8.25 (t, *J* = 5.58 Hz, 1H), 7.74 (d, *J* = 8.26 Hz, 2H), 7.66 (t, *J* = 5.78 Hz, 1H), 7.63 (d, *J* = 2.76, Hz, 1H), 7.51 - 7.46 (m, 3H), 7.25 (d, *J* = 7.52 Hz, 2H), 7.20 (d, *J* = 7.24 Hz, 1H), 7.14 (d, *J* = 8.44 Hz, 2H), 3.80 (s, 3H), 3.55 (q, *J* = 6.58 Hz 2H), 2.98 - 2.91 (m, 4H), 2.68 (t, *J* = 7.50 Hz, 2H); $^{13}$C NMR (100 MHz, DMSO-$d_6$) δ 163.6, 155.7, 144.3, 138.7, 138.3, 131.4, 129.5, 128.6, 128.3, 126.6, 126.2, 124.9, 124.3, 114.1, 56.2, 40.2, 44.0, 35.3, 34.6, 18.6.

***N*-(4-(azetidin-1-ylsulfonyl)phenethyl)-5-chloro-2-methoxybenzamide (22)** Compound **22** was prepared from compound **36** (0.39 mmol) azetidine hydrochloride (1.95 mmol) following method B in 64% yield. $^{1}$H NMR (400 MHz, DMSO-$d_6$) δ 8.29 (t, *J* = 5.52 Hz, 1H), 7.74 (d, *J* =

8.24 Hz, 2H), 7.60 - 7.56 (m, 3H), 7.50 (dd, *J* = 8.92, 2.80 Hz, 1H), 7.15 (d, *J* = 8.88 Hz, 1H), 3.83 (s, 3H), 3.64 (t, *J* = 7.66 Hz, 4H), 3.58 (q, *J* = 6.63 Hz, 2H), 2.98 (t, *J* = 7.00 Hz, 2H) 1.99 - 1.92 (m, 2H); $^{13}$C NMR (100 MHz, DMSO-$d_6$) δ 163.6, 155.7, 145.5, 131.6, 131.4, 129.8, 129.4, 128.2, 124.9, 124.3, 114.2, 56.2, 50.7, 40.1, 34.8, 14.7

**5-chloro-2-methoxy-*N*-(4-(pyrrolidin-1-ylsulfonyl)phenethyl)benzamide (23).** Compound **23** was prepared from compound **36** (0.26 mmol) and pyrrolidine (1.30 mmol) following method B in 73% yield. $^{1}$H NMR (400 MHz, DMSO-$d_6$) δ 8.25 (t, *J* = 5.68 Hz, 1H), 7.73 (d, *J* = 8.28 Hz, 2H), 7.59 (q, *J* = 2.80 Hz, 1H), 7.52 - 7.48 (m, 3H), 7.15 (d, *J* = 8.88 Hz, 1H), 3.82 (s, 3H), 3.56 (q, *J* = 6.60 Hz, 2H), 3.12 (t, *J* = 6.74 Hz, 4H), 2.94 (t, *J* = 6.98 Hz, 2H), 1.62 - 1.54 (m, 4H); $^{13}$C NMR (100 MHz, DMSO-$d_6$) δ 163.6, 155.7, 144.9, 134.2, 131.4, 129.6, 129.4, 127.3, 124.9, 124.3, 114.2, 56.2, 47.7, 40.1, 34.7, 24.6.

**5-chloro-2-methoxy-*N*-(4-(piperidin-1-ylsulfonyl)phenethyl)benzamide (24).** Compound **24** was prepared from compound **36** (0.26 mmol) and piperidine (1.30 mmol) following method B in 70% yield. $^{1}$H NMR (400 MHz, $CDCl_3$) δ 8.16 (d, J = 2.76 Hz, 1H), 7.78 (br. s., 1H), 7.71 (d, J = 8.28 Hz, 2H), 7.40 (d, J = 8.30 Hz, 1H), 7.38 (dd, J = 2.80, 8.80 Hz, 2H), 6.88 (d, J = 8.78 Hz, 1H), 3.79 (s, 3H), 3.76 (q, J = 6.78 Hz, 2H), 2.99 (t, J = 5.50 Hz, 2H), 3.01 (t, J = 6.80 Hz, 4H), 1.64 (quin, J = 5.71 Hz, 4H), 1.42 (quin, J = 5.96 Hz, 2H); $^{13}$C NMR (100 MHz, DMSO-d6) δ 163.6, 155.6, 145.0, 133.3, 131.4, 129.6, 129.4, 127.4, 124.9, 124.3, 114.1, 56.2, 46.5, 40.1, 34.7, 24.6, 22.8.

**5-chloro-2-methoxy-N-(4-(piperazin-1-ylsulfonyl)phenethyl)benzamide (25).** Compound **25** was prepared from compound **36** (0.39 mmol) and piperazine (1.95 mmol) following method B in 60% yield. $^{1}$H NMR (400 MHz, DMSO-$d_6$) δ 8.29 (t, *J* = 5.52 Hz, 1H), 7.66 (d, *J* = 8.24 Hz, 2H),

7.62 (d, $J$ = 2.76 Hz, 1H), 7.54 - 7.49 (m, 3H), 7.16 (d, $J$ = 8.92 Hz, 1H), 3.83 (s, 3H), 3.55 (q, $J$ = 7.06 Hz, 2H), 2.95 (t, $J$ = 7.06 Hz, 2H), 2.77 - 2.70 (m, 8H); $^{13}$C NMR (100 MHz, DMSO-$d_6$) δ 163.6, 156.7, 145.2, 132.8, 131.4, 129.6, 129.6, 129.5, 127.6, 124.9, 124.3, 114.2, 56.3, 46.6, 44.6, 34.7.

**5-chloro-2-methoxy-*N*-(4-(morpholinosulfonyl)phenethyl)benzamide (26).** Compound **26** was prepared from compound **36** (0.39 mmol) and morpholine (1.95 mmol) following method B in 91% yield. $^1$H NMR (400 MHz, DMSO-$d_6$) δ 8.27 (t, $J$ = 5.56 Hz, 1H), 7.68 (d, $J$ = 8.24 Hz, 2H), 7.60 (d, $J$ = 2.80 Hz, 1H), 7.55 (d, $J$ = 8.24 Hz, 2H), 7.49 (dd, $J$ = 9.01, 2.83 Hz, 1H), 7.15 (d, $J$ = 8.92 Hz, 1H), 3.82 (s, 3H), 3.62 (t, $J$ = 4.66 Hz, 4H), 3.57 (q, $J$ = 6.56 Hz, 2H), 2.96 (t, $J$ = 6.98 Hz, 2H), 2.84 (t, $J$ = 4.62 Hz, 4H); $^{13}$C NMR (100 MHz, DMSO-$d_6$) δ 163.6, 155.7, 145.5, 132.3, 131.4, 129.7, 129.4, 127.7, 124.9, 124.3, 114.1, 65.2, 56.2, 45.9, 40.1, 34.7.

**5-chloro-2-methoxy-*N*-(3-(4-(*N*-methylsulfamoyl)phenyl)propyl)benzamide (27).** Compound **27** was prepared from **41** (0.37 mmol) and methylamine HCl (0.19 mmol) following Method B in 72% yield. $^1$H NMR (400 MHz, DMSO-$d_6$) δ 8.29 (t, $J$ = 5.30 Hz, 1H), 7.70 (d, $J$ = 8.28 Hz, 2H), 7.64 (d, $J$ = 2.76 Hz, 1H), 7.51 (dd, $J$ = 9.91, 2.91 Hz, 1H), 7.47 (d, $J$ = 8.24 Hz, 2H), 7.37 (q, $J$ = 5.01 Hz, 1H), 7.17 (d, $J$ = 8.88 Hz, 1H), 3.88 (s, 3H), 3.28 (q, $J$ = 6.18 Hz, 2H), 2.73 (t, $J$ = 7.66 Hz, 2H), 2.40 (t, $J$ = 5.04 Hz, 3H), 1.85 (quin, $J$ = 7.32 Hz, 2H); $^{13}$C NMR (100 MHz, DMSO-$d_6$) δ 163.8, 155.6, 146.7, 136.8, 131.2, 129.3, 129.0 125.7, 125.5, 124.2, 114.1, 56.3, 38.7, 32.3, 30.3 28.6.

**5-chloro-2-methoxy-*N*-(4-(4-(*N*-methylsulfamoyl)phenyl)butyl)benzamide (28).** Compound **28** was prepared from **42** (0.37 mmol) and methylamine HCl (0.19 mmol) following Method B in 84% yield. $^1$H NMR (400 MHz, DMSO-$d_6$) δ 8.24 (t, $J$ = 5.54 Hz, 1H), 7.70 (d, $J$ = 8.24 Hz, 2H),

7.62 (d, *J* = 2.76 Hz, 1H), 7.50 (dd, *J* = 8.66, 2.62 Hz, 1H), 7.45 (d, *J* = 8.20 Hz, 2H), 7.35 (q, *J* = 5.05 Hz, 1H), 7.16 (d, *J* = 8.88 Hz, 1H), 3.85 (s, 3H), 3.29 (q, *J* = 6.67 Hz, 2H), 2.71 (t, *J* = 7.50 Hz, 2H), 2.40 (d, *J* = 5.04 Hz, 3H), 1.65 (quin, *J* =8.15 Hz, 2H), 1.54 (quin, *J* =7.06 Hz, 2H); $^{13}$C NMR (100 MHz, DMSO-$d_6$) δ 163.7, 155.6, 147.2, 136.7, 131.2, 129.3, 129.0, 126.7, 125.5, 124.3, 114.1, 56.3, 38.8, 34.5, 28.7, 28.6, 27.9.

**2-phenethylisoindoline-1,3-dione (30).** Phthalic anhydride (103.20 mmol) and 2-phenylethylamine **29** (82.50 mmol) were added to acetic acid (30 mL), and refluxed for 3 h. The solution was cooled to room temperature and was poured into ice-water. The precipitate was filtered and purified by recrystallization in ethanol to give **30** as a white solid, **(**17.25 g, 33%). $^{1}$H NMR (400 MHz, DMSO-$d_6$) δ 7.84 - 7.81 (m, 4H), 7.27 - 7.16 (m, 5H), 3.82 (t, *J* = 7.36 Hz, 2H), 2.93 (t, *J* = 7.34 Hz, 2H); $^{13}$C NMR (100 MHz, DMSO-$d_6$) δ 167.6, 138.2, 134.4, 131.5, 128.6, 128.4 126.4, 122.3, 38.8, 33.6

**Method A. 4-(2-(1,3-dioxoisoindolin-2-yl)ethyl)benzenesulfonyl chloride (31).** To the solution of **30** (59.74 mmol) in dichloromethane (DCM) was added chlorosulfonic acid (15 mL) at -20 ºC. Then the solution was heated to 60 ºC for 1 h. The solution was cooled to room temperature and poured onto crushed ice. The product was extracted into DCM, concentrated, and purified by column chromatography to give **31** as a white solid (17.05 g, 82%). $^{1}$H NMR (400 MHz, DMSO-$d_6$) δ 7.83 - 7.82 (m, 4H), 7.49 (d, *J* = 7.55 Hz, 2H), 7.16 (d, *J* = 7.56 Hz, 2H), 3.81 (t, *J* = 7.16 Hz, 2H), 2.92 (t, *J* = 7.16 Hz, 2H); $^{13}$C NMR (100 MHz, DMSO-$d_6$) δ 167.6, 146.1, 138.7, 134.4, 131.4, 127.9, 125.6, 123.0, 38.6, 33.4.

**Method B. 4-(2-(1,3-dioxoisoindolin-2-yl)ethyl)-*N*-methylbenzenesulfonamide (32).** To the solution of compound **31** (10.40 mmol) in DCM (200 mL) was added methylamine (52.00 mmol)

and trimethylamine ($Et_3N$) (52.00 mmol). The solution was stirred overnight at room temperature. The reaction was diluted with $H_2O$ and the product was extracted into DCM, concentrated, and purified by column chromatography to give **32** (3.36 g, 84%) as a white solid. $^1$H NMR (400 MHz, DMSO-$d_6$) δ 7.83- 7.82 (m, 4H), 7.65 (d, $J$ = 8.28 Hz, 2H), 7.44 (d, $J$ = 8.24 Hz, 2H), 7.35 (q, $J$ = 5.01 Hz, 1H), 3.86 (t, $J$ = 7.12 Hz, 2H), 3.02 (t, $J$ = 7.06 Hz, 2H), 2.35 (d, $J$ = 5.04 Hz, 3H); $^{13}$C NMR (100 MHz, DMSO-$d_6$) δ 167.6, 143.2, 137.3, 134.4, 131.4, 129.5, 126.8, 123.0, 38.4, 33.5, 28.5.

**4-(2-aminoethyl)-*N*-methylbenzenesulfonamide (33).** Hydrazine, (30.00 mmol) was added dropwise to a stirring solution of **32** (6.01 mmol) in EtOH (10 mL). After addition, the solution was heated to 60 $^o$C for 12 h. The precipitate was then washed with hexane. The filtrate was collected and concentrated under reduced pressure. The crude product was then purified by column chromatography to give **33** as a yellow liquid (1.01 g, 79%). $^1$H NMR (400 MHz, DMSO-$d_6$) δ 7.69 (d, $J$ = 8.32 Hz, 2H), 7.43 (d, $J$ = 8.32 Hz, 2H), 2.80 (t, $J$ = 6.54 Hz, 2H), 2.72 (t, $J$ = 6.60 Hz, 2H), 2.40 (s, 3H); $^{13}$C NMR (100 MHz, DMSO-$d_6$) δ 145.5, 136.8, 129.3, 126.6, 43.1, 39.4, 28.6.

**Method C. 5-chloro-2-methoxy-N-phenethylbenzamide (35).** 2-Methoxy-5-chloro-benzoic acid 34 (0.47 mmol) and $Et_3N$ (0.93 mmol) were dissolved in DCM (4 mL) and the mixture was cooled to 0 ºC. To this solution, 1-ethyl-3-(3-dimethylaminopropyl)carbodiimide (EDC, 0.70 mmol) and hydroxybenzotriazole (HOBt, 0.70 mmol) were added. After 1 h, **29** (0.47 mmol) was added and the reaction was allowed to room temperature overnight. The solution was diluted with DCM and $H_2O$, and was extracted into DCM. The combined organic phase was concentrated and purified by column chromatography to give **35** as a white powder (37% yield). $^1$H NMR (400 MHz, DMSO-$d_6$) δ 8.22 (d, $J$=3.04 Hz, 1H), 7.66 (br. s., 1H), 7.50 (dd, $J$ = 8.80, 3.00 Hz, 1H), 7.32 (d, $J$

= 7.22 Hz, 2H), 7.28 (d, *J* = 8.03 Hz, 2H), 7.24 - 7.20 (m, 1H), 7.16 (d, *J* = 9.46 Hz, 1H), 3.81 (s, 3H), 3.54 (q, *J* = 7.06 Hz, 2H), 2.85 (t, *J* = 6.20 Hz, 2H); $^{13}$C NMR (100 MHz, DMSO-$d_6$) δ 163.4, 155.7, 139.4, 131.5, 129.6, 128.7, 128.3, 126.1, 124.7, 124.3, 114.1, 56.2, 40.7, 34.9.

**4-(2-[(5-chloro-2-methoxyphenyl)formamido]ethyl)benzene-1- sulfonyl chloride (36).** Compound **36** was prepared from compound **35** (9.50 mmol) following Method A in 62% yield. $^1$H NMR (400 MHz, DMSO-$d_6$) δ 8.20 (br. s., 1H), 7.66 (s, 1H), 7.56 (d, *J* = 8.28 Hz, 2H), 7.50 (dd, *J* = 8.78, 2.76 Hz, 1H), 7.22 (d, *J* = 8.53 Hz, 2H), 7.16 (d, *J* = 9.04 Hz, 1H), 3.80 (s, 3H), 3.51 (q, *J* = 7.30 Hz, 2H), 2.84 (t, *J* = 6.80 Hz, 2H); $^{13}$C NMR (100 MHz, DMSO-$d_6$) δ 163.5, 155.7, 146.1, 139.8, 131.5, 129.5, 128.0, 125.6, 124.7, 124.3, 114.2, 56.2, 40.6, 34.6.

**5-chloro-2-methoxy-N-phenpropyllbenzamide (39).** Compound **39** was prepared from **34** (5.36 mmol) and **37** (5.36 mmol) following Method C in 59% yield. $^1$H NMR (400 MHz, DMSO-$d_6$) δ 8.26 (t, *J* = 5.28 Hz, 1H), 7.63 (d, *J* = 2.80 Hz, 1H), 7.51 (dd, *J* = 8.92, 2.91 Hz, 1H), 7.32 - 7.16 (m, 6H), 3.88 (s, 3H), 3.28 (q, *J* = 6.62 Hz, 2H), 2.64 (t, *J* = 7.68 Hz, 2H), 1.82 (quin, *J* = 7.37 Hz, 2H); $^{13}$C NMR (100 MHz, DMSO-$d_6$) δ 163.4, 155.7, 139.4, 131.5, 129.6, 128.7, 128.3, 126.1, 124.7, 124.3, 114.1, 56.2, 40.7, 34.9.

**5-chloro-2-methoxy-*N*-(4-(4-(*N*-methylsulfamoyl)phenyl)butyl)benzamide (40).** Ccompound **40** was prepared from **34** (5.36 mmol) and **38** (5.36 mmol) following Method C in 73% yield. $^1$H NMR (400 MHz, DMSO-$d_6$) δ 8.07 (d, *J* = 5.73 Hz, 1H), 7.46 (d, *J* = 2.82 Hz, 1H), 7.33 (dd, *J* = 9.29, 3.00 Hz, 1H), 7.13 - 6.97 (m, 6H), 3.68 (s, 3H), 3.12 (q, *J* = 6.67 Hz, 2H), 2.46 (t, *J* = 7.73 Hz, 2H), 1.53 - 1.33 (m, 4H)$^{13}$C NMR (100 MHz, DMSO-$d_6$) δ 164.1, 156.1, 142.7, 131.7, 129.8, 128.8, 128.7, 126.2, 126.1, 126.0, 124.7, 114.5, 56.7, 39.3, 35.3, 29.2, 28.9.

**4-(3-(5-chloro-2-methoxybenzamido)propyl)benzenesulfonyl chloride (41).** Ccompound **41**

was prepared from **39** (3.18 mmol) following Method A in 53% yield. $^1$H NMR (400 MHz, DMSO-$d_6$) δ 8.26 (t, $J$ = 5.46 Hz, 1H), 7.63 (d, $J$ = 2.80 Hz, 1H), 7.54 (d, $J$ = 8.12 Hz, 2H), 7.48 (dd, $J$ = 8.91, 2.92 Hz, 1H), 7.19 (d, $J$ = 8.16 Hz, 2H), 7.16 (d, $J$ = 8.92 Hz, 1H), 3.87 (s, 3H), 3.27 (q, $J$ = 6.56 Hz, 2H), 2.63 (t, $J$ = 7.66 Hz, 2H), 1.80 (quin, $J$ = 7.34 Hz, 2H); $^{13}$C NMR (100 MHz, DMSO-$d_6$) δ 163.8, 155.6, 145.4, 142.3, 131.2, 129.3, 127.6, 125.6, 125.5, 124.24, 114.1, 56.3, 38.7, 32.6, 30.7.

**4-(4-(5-chloro-2-methoxybenzamido)butyl)benzenesulfonyl chloride (42).** Compound **42** was prepared from **40** (3.10 mmol) following Method A in 38% yield. $^1$H NMR (400 MHz, DMSO-$d_6$) δ 8.21 (t, $J$ = 5.54 Hz, 1H), 7.61 (d, $J$ = 2.80 Hz, 1H), 7.52 (d, $J$ = 8.08 Hz, 2H), 7.48 (dd, $J$ = 8.90, 2.80 Hz, 1H), 7.17 - 7.13 (m, 3H), 3.84 (s, 3H), 3.27 (q, $J$ = 6.47 Hz, 2H), 2.61 (t, $J$ = 7.40 Hz, 2H), 1.64 - 1.48 (m, 4H),; $^{13}$C NMR (100 MHz, DMSO-$d_6$) δ 163.7, 155.7, 145.4, 142.7, 131.2, 129.3, 127.5, 125.5, 124.4, 114.1, 56.3, 38.8, 34.4, 28.5, 28.2.

**Biological assays.**

**Cells**: J774A.1 murine macrophage cells were purchased from American Type Cell Culture (ATCC, Manassas, VA) and were cultured in Dulbecco's Modified Eagle Medium (DMEM) with 10% fetal bovine serum (FBS), 1% penicillin/streptomycin.

**IL-1β release assays.** J774A.1 cells were plated into a 96- well plate ($1 \times 10^5$ cells/well) for 24 h in growth medium. Cells were primed with Escherichia coli 0111:B4 LPS (Sigma-Aldrich) (final concentration: 1 μg/mL) for 4.5 h. Next, test compounds were added for 30 min. ATP (5 mM) was added at the same time when compounds were added to induce NLRP3 inflammasome activation. After 30 min, the supernatants were collected and the level of IL-1β was measured with

a mouse IL-1β ELISA kit following the manufacturer's instructions. BMDMs were similarly treated as described with J774A.1 cell line followed by ELISA analysis for IL-β production.

**Inhibition on the NLRC4 and AIM2 inflammasomes.** J774A.1 cells were plated into a 96-well plate ($1 \times 10^5$ cells/well) for 24 h in growth medium. Cells were treated with LPS (1 μg/mL) and test compounds for 1 h. Flagellin or poly-deoxyadenylic-deoxythymidylic acid sodium salt (Poly(dA:dT)) was used to induce the formation of the NLRC4 and the AIM2 inflammasomes. Flagellin (Enzo Life Sciences, Farmingdale, NY), isolated from *Salmonella typhimurium* strain 14028, was added in DMEM (Invitrogen) without fetal bovine serum (FBS) to the plate (1 μg/mL) and allowed to incubate for 6 h. Flagellin cell-transfection was accomplished utilizing the Polyplus transfection kit (PULSin, New York, NY). For AIM2 activation, cells were incubated with Poly(dA:dT) (4 μg/ml) (InvivoGen, San Diego, CA) for 8 h. The supernatants were collected and levels of IL-1β were measured with a mouse IL-1β ELISA kit following the manufacturer's instructions.

**Animals:** All animal experiments were conducted under the guidelines of the "Guide for the care and use of laboratory animals" published by National Institutes of Health (revised 2011). ICR mice (8-12 weeks old) were purchased from Harlan Laboratories (Charles River, MA). C57BL/6 mice were purchased from the National Cancer Institute (Bethesda, MD). APP/PS1 female transgenic mice (B6C3-Tg (APPswe, PSEN1dE9)85Dbo/Mmjax) and matching wild type female mice were purchased from the Jackson Laboratory.

**Experimental model of AMI.** Briefly, ICR mice were anesthetized using pentobarbital (50-70 mg/kg, Sigma-Aldrich, St. Louis, MO) followed by orotracheal intubation. After placing them in the right lateral decubitus position, the mice were subjected to left thoracotomy, pericardiectomy,

and the proximal left coronary artery was ligated for 30 min or 75 min and then released (I/R model). Different groups of mice were treated with the compound or a matching volume of vehicle (0.1mL) (N=6 in each group). Myocardial damage was determined by measuring serum troponin I level at 24 h after surgery and with pathology assessment of viability. Briefly, mice were anesthetized and the blood was drawn from the inferior vena cava and collected in Vacutainer tubes (BD Vacutainer, Franklin Lakes, NJ) for serum isolation. Mouse troponin I levels were determined by ELISA (Life Diagnostic Inc., West Chester, PA). Infarct size was measured at 24 h after induction of ischemia using TTC (Sigma-Aldrich) to stain viable myocardium.

**LPS challenge *in vivo* and compound treatments.** C57BL/6 mice were injected intraperitoneally (i.p.) with 20 mg/kg LPS (Sigma-Aldrich) or PBS one hour after compound or vehicle treatment. 2.5 h after LPS injection, serum levels of IL-1β were measured by ELISA.

**Studies in APP/PS1 mice.** At the age of 7 months old, animals were randomly divided into the following experimental groups: WT: vehicle group (n=4), JC124 treatment group (n=6). APP/PS1 mice: vehicle group (n=5), JC124 treatment group (n=7). For i.p., JC124 was dissolved in 10% DMSO with PEG-100. For oral dosing, JC124 was dissolved in 2% DMSO in corn oil. Starting at the age of 7 months old, animals first received i.p. injection of JC124 or vehicle single daily for 5 days (Monday through Friday), then changed to oral dosing single daily for 5 days during weekdays for 7 weeks. After completing the 8 weeks treatment, animals were tested on cognitive functions using NOR and MWM tests.

**Abbreviations**

AD, Alzheimer's disease; AMI, acute myocardial infarction; Aβ, Amyloid-β; ASC, apoptosis-associated speck-like protein containing a CARD; ATP, adenosine triphosphate; Aβ,

beta-amyloid; BMDMs, mouse bone marrow derived macrophages; CAPS, cryopyrin -associated periodic syndrome; DCM, Dichloromethane; DI, discrimination index; DMEM, Dulbecco's Modified Eagle Medium; EDCI, *N*-(3-(dimethylamino)propyl)-*N*-ethyl- carbodiimide hydrochloride; ELISA, enzyme-linked immunosorbent assay; FBS, fetal bovine serum; HOBt, hydroxybenzotriazole; IL-1β, interleukin-1β; LPS, lipopolysaccharide; MOA, mechanisms of action; MS, multiple sclerosis; MWM, Morris Water Maze; NLRP3, NOD-like receptor family pyrin-domain-containing 3; NLRP3Is, NLRP3 inflammasome inhibitors; NOR, Novel Object Recognition; PBS, phosphate-buffered saline; Poly(dA:dT), poly-deoxyadenylic- deoxythymidylic acid sodium salt; PMA, Phosphomolybdic acid; RIG-I, retinoic acid-inducible gene I; SAR, structure activity relationship; TBI, traumatic brain injury; TFA, trifluoroacetic acid; TMS, Tetramethylsilane; TTC, triphenyltetrazolium chloride; $Et_3N$, trimethylamine.

**Author Information**

Corresponding Author:

Shijun Zhang, Ph.D., Tel: 804-6288266, Fax: 804-8287625, E-mail: szhang2@vcu.edu

ORCID:

Shijun Zhang: 0000-0001-9732-5925

**Acknowledgements**

The work was supported in part by the NIA of the NIH under award number R01AG041161 and R01AG058673 (SZ), Alzheimer's Drug Discovery Foundation 20150601 (SZ), Award No. 18-2 from the Commonwealth of Virginia's Alzheimer's and Related Disease Research Award Fund administered by the Center on Aging, School of Allied Health Professions, Virginia Commonwealth University (SZ), VCU Presidential Research Quest Fund (SZ).

**Supporting Information**

Molecular formula strings (CSV)

**References**

(1) Martinon, F.; Burns, K.; Tschopp, J. The Inflammasome: A Molecular Platform Triggering Activation of Inflammatory Caspases and Processing of Proil-Beta. *Mol. Cell*. **2002**, *10*, 417-426.

(2) Latz, E.; Xiao, T. S.; Stutz, A. Activation and Regulation of the Inflammasomes. *Nat. Rev. Immunol*. **2013**, *13*, 397-411.

(3) Schroder, K.; Tschopp, J. The Inflammasomes. *Cell*. **2010**, *140*, 821-832.

(4) Shao, B. Z.; Xu, Z. Q.; Han, B. Z.; Su, D. F.; Liu, C. Nlrp3 Inflammasome and Its Inhibitors: A Review. *Front. Pharmacol*. **2015**, *6*, 262-271.

(5) Shi, H.; Wang, Y.; Li, X.; Zhan, X.; Tang, M.; Fina, M.; Su, L.; Pratt, D.; Bu, C. H.; Hildebrand, S.; Lyon, S.; Scott, L.; Quan, J.; Sun, Q.; Russell, J.; Arnett, S.; Jurek, P.; Chen, D.; Kravchenko, V. V.; Mathison, J. C.; Moresco, E. M.; Monson, N. L.; Ulevitch, R. J.; Beutler, B. Nlrp3 Activation and Mitosis Are Mutually Exclusive Events Coordinated by Nek7, a New Inflammasome Component. *Nat. Immunol*. **2016**, *17*, 250-258.

(6) He, Y.; Zeng, M. Y.; Yang, D.; Motro, B.; Nunez, G. Nek7 Is an Essential Mediator of Nlrp3 Activation Downstream of Potassium Efflux. *Nature*. **2016**, *530*, 354-357.

(7) Schmid-Burgk, J. L.; Chauhan, D.; Schmidt, T.; Ebert, T. S.; Reinhardt, J.; Endl, E.; Hornung, V. A Genome-Wide Crispr (Clustered Regularly Interspaced Short Palindromic Repeats) Screen Identifies Nek7 as an Essential Component of Nlrp3 Inflammasome Activation. *J. Biol. Chem*. **2016**, *291*, 103-109.

(8) De Nardo, D.; Latz, E. Nlrp3 Inflammasomes Link Inflammation and Metabolic Disease. *Trends Immunol*. **2011**, *32*, 373-379.

(9) Hoffman, H. M.; Mueller, J. L.; Broide, D. H.; Wanderer, A. A.; Kolodner, R. D. Mutation of a New Gene Encoding a Putative Pyrin-Like Protein Causes Familial Cold Autoinflammatory Syndrome and Muckle-Wells Syndrome. *Nat. Genet*. **2001**, *29*, 301-305.

(10) Menu, P.; Vince, J. E. The Nlrp3 Inflammasome in Health and Disease: The Good, the Bad and the Ugly. *Clin. Exp. Immunol*. **2011**, *166*, 1-15.

(11) Peelen, E.; Damoiseaux, J.; Muris, A. H.; Knippenberg, S.; Smolders, J.; Hupperts, R.; Thewissen, M. Increased Inflammasome Related Gene Expression Profile in Pbmc May Facilitate T Helper 17 Cell Induction in Multiple Sclerosis. *Mol. Immunol*. **2015**, *63*, 521-529.

(12) Choi, A. J.; Ryter, S. W. Inflammasomes: Molecular Regulation and Implications for Metabolic and Cognitive Diseases. *Mol. Cells*. **2014**, *37*, 441-448.

(13) Couturier, J.; Stancu, I. C.; Schakman, O.; Pierrot, N.; Huaux, F.; Kienlen-Campard, P.; Dewachter, I.; Octave, J. N. Activation of Phagocytic Activity in Astrocytes by Reduced Expression of the Inflammasome Component Asc and Its Implication in a Mouse Model of Alzheimer Disease. *J. Neuroinflammation*. **2016**, *13*, 20.

(14) Ting, J. P.; Kastner, D. L.; Hoffman, H. M. Caterpillers, Pyrin and Hereditary Immunological Disorders. *Nat. Rev. Immunol*. **2006**, *6*, 183-195.

(15) Freeman, L. C.; Ting, J. P. The Pathogenic Role of the Inflammasome in Neurodegenerative Diseases. *J. Neurochem*. **2016**, *136 Suppl 1*, 29-38.

(16) Inoue, M.; Shinohara, M. L. Nlrp3 Inflammasome and Ms/Eae. *Autoimmune Dis*. **2013**, *2013*, 859145.

(17) Heneka, M. T.; Kummer, M. P.; Stutz, A.; Delekate, A.; Schwartz, S.; Vieira-Saecker, A.; Griep, A.; Axt, D.; Remus, A.; Tzeng, T. C.; Gelpi, E.; Halle, A.; Korte, M.; Latz, E.; Golenbock,

D. T. Nlrp3 Is Activated in Alzheimer's Disease and Contributes to Pathology in App/Ps1 Mice. *Nature*. **2013**, *493*, 674-678.

(18) Saresella, M.; La Rosa, F.; Piancone, F.; Zoppis, M.; Marventano, I.; Calabrese, E.; Rainone, V.; Nemni, R.; Mancuso, R.; Clerici, M. The Nlrp3 and Nlrp1 Inflammasomes Are Activated in Alzheimer's Disease. *Mol. Neurodegener*. **2016**, *11*, 23.

(19) Walsh, J. G.; Muruve, D. A.; Power, C. Inflammasomes in the CNS. *Nat. Rev. Neurosci*. **2014**, *15*, 84-97.

(20) Venegas, C.; Kumar, S.; Franklin, B.S.; Dierkes, T.; Brinkschulte, R.; Tejera, D.; Vieira-Saecker, A.; Schwartz, S.; Santarelli, F.; Kummer, M.P.; Griep, A.; Gelpi, E.; Beilharz, M.; Riedel, D.; Golenbock, D.T.; Geyer, M.; Walter, J.; Latz, E.; Heneka, M.T. Microglia-Derived ASC Specks Cross-Seed Amyloid-β in Alzheimer's Disease. *Nature* **2017**, *552*, 355-361.

(21) Halle, A.; Hornung, V.; Petzold, G. C.; Stewart, C. R.; Monks, B. G.; Reinheckel, T.; Fitzgerald, K. A.; Latz, E.; Moore, K. J.; Golenbock, D. T. The Nalp3 Inflammasome Is Involved in the Innate Immune Response to Amyloid-Beta. *Nat. Immunol*. **2008**, *9*, 857-865.

(22) Zhu, S. G.; Sheng, J. G.; Jones, R. A.; Brewer, M. M.; Zhou, X. Q.; Mrak, R. E.; Griffin, W. S. Increased Interleukin-1beta Converting Enzyme Expression and Activity in Alzheimer Disease. *J. Neuropathol. Exp. Neurol*. **1999**, *58*, 582-587.

(23) Toldo, S.; Mezzaroma, E.; Mauro, A. G.; Salloum, F.; Van Tassell, B. W.; Abbate, A. The Inflammasome in Myocardial Injury and Cardiac Remodeling. *Antioxid. Redox. Signal*. **2015**, *22*, 1146-1161.

(24) Toldo, S.; Mezzaroma, E.; McGeough, M. D.; Pena, C. A.; Marchetti, C.; Sonnino, C.; Van Tassell, B. W.; Salloum, F. N.; Voelkel, N. F.; Hoffman, H. M.; Abbate, A. Independent Roles of

the Priming and the Triggering of the Nlrp3 Inflammasome in the Heart. *Cardiovasc. Res*. **2015**, *105*, 203-212.

(25) Mezzaroma, E.; Toldo, S.; Farkas, D.; Seropian, I. M.; Van Tassell, B. W.; Salloum, F. N.; Kannan, H. R.; Menna, A. C.; Voelkel, N. F.; Abbate, A. The Inflammasome Promotes Adverse Cardiac Remodeling Following Acute Myocardial Infarction in the Mouse. *Proc. Natl. Acad. Sci. U S A*. **2011**, *108*, 19725-19730.

(26) Syed, F. M.; Hahn, H. S.; Odley, A.; Guo, Y.; Vallejo, J. G.; Lynch, R. A.; Mann, D. L.; Bolli, R.; Dorn, G. W., 2nd. Proapoptotic Effects of Caspase-1/Interleukin-Converting Enzyme Dominate in Myocardial Ischemia. *Circ. Res*. **2005**, *96*, 1103-1109.

(27) Kawaguchi, M.; Takahashi, M.; Hata, T.; Kashima, Y.; Usui, F.; Morimoto, H.; Izawa, A.; Takahashi, Y.; Masumoto, J.; Koyama, J.; Hongo, M.; Noda, T.; Nakayama, J.; Sagara, J.; Taniguchi, S.; Ikeda, U. Inflammasome Activation of Cardiac Fibroblasts Is Essential for Myocardial Ischemia/Reperfusion Injury. *Circulation*. **2011**, *123*, 594-604.

(28) Sandanger, O.; Ranheim, T.; Vinge, L. E.; Bliksoen, M.; Alfsnes, K.; Finsen, A. V.; Dahl, C. P.; Askevold, E. T.; Florholmen, G.; Christensen, G.; Fitzgerald, K. A.; Lien, E.; Valen, G.; Espevik, T.; Aukrust, P.; Yndestad, A. The Nlrp3 Inflammasome Is up-Regulated in Cardiac Fibroblasts and Mediates Myocardial Ischaemia-Reperfusion Injury. *Cardiovasc. Res*. **2013**, *99*, 164-174.

(29) Merkle, S.; Frantz, S.; Schon, M. P.; Bauersachs, J.; Buitrago, M.; Frost, R. J.; Schmitteckert, E. M.; Lohse, M. J.; Engelhardt, S. A Role for Caspase-1 in Heart Failure. *Circ. Res*. **2007**, *100*, 645-653.

(30) Dinarello, C. A.; Simon, A.; van der Meer, J. W. Treating Inflammation by Blocking

Interleukin-1 in a Broad Spectrum of Diseases. *Nat. Rev. Drug Discov*. **2012**, *11*, 633-652.

(31) Baldwin, A. G.; Brough, D.; Freeman, S. Inhibiting the Inflammasome: A Chemical Perspective. *J. Med. Chem*. **2016**, *59*, 1691-1710.

(32) Lamkanfi, M.; Mueller, J. L.; Vitari, A. C.; Misaghi, S.; Fedorova, A.; Deshayes, K.; Lee, W. P.; Hoffman, H. M.; Dixit, V. M. Glyburide Inhibits the Cryopyrin/Nalp3 Inflammasome. *J. Cell Biol*. **2009**, *187*, 61-70.

(33) Marchetti, C.; Chojnacki, J.; Toldo, S.; Mezzaroma, E.; Tranchida, N.; Rose, S. W.; Federici, M.; Van Tassell, B. W.; Zhang, S.; Abbate, A. A Novel Pharmacologic Inhibitor of the Nlrp3 Inflammasome Limits Myocardial Injury after Ischemia-Reperfusion in the Mouse. *J. Cardiovasc. Pharmacol*. **2014**, *63*, 316-322.

(34) Marchetti, C.; Toldo, S.; Chojnacki, J.; Mezzaroma, E.; Liu, K.; Salloum, F. N.; Nordio, A.; Carbone, S.; Mauro, A. G.; Das, A.; Zalavadia, A. A.; Halquist, M. S.; Federici, M.; Van Tassell, B. W.; Zhang, S.; Abbate, A. Pharmacologic Inhibition of the Nlrp3 Inflammasome Preserves Cardiac Function after Ischemic and Nonischemic Injury in the Mouse. *J. Cardiovasc. Pharmacol*. **2015**, *66*, 1-8.

(35) Toldo, S.; Marchetti, C.; Mauro, A. G.; Chojnacki, J.; Mezzaroma, E.; Carbone, S.; Zhang, S.; Van Tassell, B.; Salloum, F. N.; Abbate, A. Inhibition of the Nlrp3 Inflammasome Limits the Inflammatory Injury Following Myocardial Ischemia-Reperfusion in the Mouse. *Int. J. Cardiol*. **2016**, *209*, 215-220.

(36) Yin, J.; Zhao, F.; Chojnacki, J. E.; Fulp, J.; Klein, W. L.; Zhang, S.; Zhu, X. Nlrp3 Inflammasome Inhibitor Ameliorates Amyloid Pathology in a Mouse Model of Alzheimer's Disease. *Mol. Neurobiol*. **2018**, *55*, 1977-1987.

(37) Chishti, M. A.; Yang, D. S.; Janus, C.; Phinney, A. L.; Horne, P.; Pearson, J.; Strome, R.; Zuker, N.; Loukides, J.; French, J.; Turner, S.; Lozza, G.; Grilli, M.; Kunicki, S.; Morissette, C.; Paquette, J.; Gervais, F.; Bergeron, C.; Fraser, P. E.; Carlson, G. A.; George-Hyslop, P. S.; Westaway, D. Early-Onset Amyloid Deposition and Cognitive Deficits in Transgenic Mice Expressing a Double Mutant Form of Amyloid Precursor Protein 695. *J. Biol. Chem*. **2001**, *276*, 21562-21570.

(38) Dudal, S.; Krzywkowski, P.; Paquette, J.; Morissette, C.; Lacombe, D.; Tremblay, P.; Gervais, F. Inflammation Occurs Early During the Abeta Deposition Process in Tgcrnd8 Mice. *Neurobiol. Aging*. **2004**, *25*, 861-871.

(39) Borchelt, D. R.; Ratovitski, T.; van Lare, J.; Lee, M. K.; Gonzales, V.; Jenkins, N. A.; Copeland, N. G.; Price, D. L.; Sisodia, S. S. Accelerated Amyloid Deposition in the Brains of Transgenic Mice Coexpressing Mutant Presenilin 1 and Amyloid Precursor Proteins. *Neuron*. **1997**, *19*, 939-945.

(40) Toldo, S.; Mezzaroma, E.; Abbate, A. Interleukin-1 Blockade in Acute Myocardial Infarction and Heart Failure: Ready for Clinical Translation. *Transl Med*. **2012**, *3*, e114.

(41) Guo, C.; Fulp, J. W.; Jiang, Y.; Li, X.; Chojnacki, J. E.; Wu, J.; Wang, X. Y.; Zhang, S. Development and Characterization of a Hydroxyl-Sulfonamide Analogue, 5-Chloro-N-[2-(4-Hydroxysulfamoyl-Phenyl)-Ethyl]-2-Methoxy-Benzamide, as a Novel Nlrp3 Inflammasome Inhibitor for Potential Treatment of Multiple Sclerosis. *ACS Chem. Neurosci*. **2017**, *8*, 2194-2201.

(42) Coll, R. C.; Robertson, A. A.; Chae, J. J.; Higgins, S. C.; Munoz-Planillo, R.; Inserra, M. C.; Vetter, I.; Dungan, L. S.; Monks, B. G.; Stutz, A.; Croker, D. E.; Butler, M. S.; Haneklaus, M.;

Sutton, C. E.; Nunez, G.; Latz, E.; Kastner, D. L.; Mills, K. H.; Masters, S. L.; Schroder, K.; Cooper, M. A.; O'Neill, L. A. A Small-Molecule Inhibitor of the Nlrp3 Inflammasome for the Treatment of Inflammatory Diseases. *Nat. Med*. **2015**, *21*, 248-255.

(43) He, Y.; Franchi, L.; Nunez, G. Tlr Agonists Stimulate Nlrp3-Dependent Il-1beta Production Independently of the Purinergic P2x7 Receptor in Dendritic Cells and in Vivo. *J. Immunol*. **2013**, *190*, 334-339.

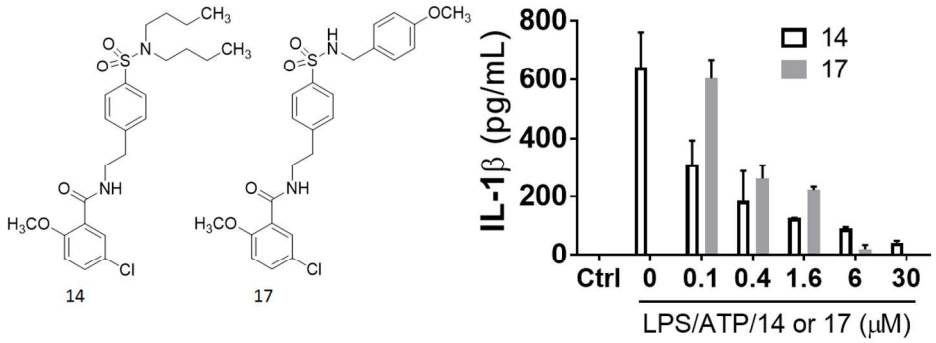


For Table of Contents Use Only

323x124mm (300 x 300 DPI)